Title

STABLE-FLOW FREE-BOUNDARY MIGRATION AND FRACTIONATION OF CELL MIXTURES: SEDIMENTATION AND ELECTROPHORESIS

Author

Mel, Howard C.

Publication Date

1963-01-23

UCRL-10640

University of California

Ernest O. Lawrence Radiation Laboratory

STABLE-FLOW FREE-BOUNDARY MIGRATION AND FRACTIONATION OF CELL MIXTURES: SEDIMENTATION AND ELECTROPHORESIS

Berkeley, California

DISCLAIMER

Research and Development

UCRL-10640
UC-48 Biology and Medicine
TID-4500 (18th Ed.)

UNIVERSITY OF CALIFORNIA

Lawrence Radiation Laboratory
Berkeley, California

Contract No. W-7405-eng-48

STABLE-FLOW FREE-BOUNDARY MIGRATION AND FRACTIONATION OF CELL MIXTURES: SEDIMENTATION AND ELECTROPHORESIS

Howard C. Mel

Division of Medical Physics
and Donner Laboratory of Biophysics and Medical Physics,
University of California, Berkeley, California

January 23, 1963

Printed in USA. Price $2.00. Available from the
Office of Technical Services
U. S. Department of Commerce
Washington 25, D.C.

STABLE-FLOW FREE-BOUNDARY MIGRATION AND FRACTIONATION OF CELL MIXTURES: SEDIMENTATION AND ELECTROPHORESIS

Contents

STABLE-FLOW FREE-BOUNDARY MIGRATION AND FRACTIONATION OF CELL MIXTURES: SEDIMENTATION AND ELECTROPHORESIS

Howard C. Mel

Division of Medical Physics
and Donner Laboratory of Biophysics and Medical Physics,
University of California, Berkeley, California

January 23, 1963

ABSTRACT

A number of analytical and preparative problems of complex biological mixtures, requiring speed and mildness of handling, large capacity, and high resolution, can be advantageously attacked by the stable-flow free boundary (STAFLO) method. Experimental and theoretical aspects of STAFLO migration, fractionation, and concentration are analyzed, with particular reference to cell mixtures. Combination gradient profiles of composition, conductivity, pH, etc. can be established almost arbitrarily in a steady-state manner, without the usual gradient mixing devices.

The solution to the basic problem of stabilizing flows, without the use of an anticonvective supporting medium, is discussed in detail. The basis and nature of stable flow in a broad sense relate to: (a) self-balancing hydrodynamic feedback, (b) a special kind of laminar flow, and (c) density-gradient stability. The feedback depends on both hydrostatic (multiple siphon) and hydrodynamic (velocity-viscosity) considerations. With the maximum operating Reynolds number of 17, there appears ample safety margin before onset of turbulence. The manner in which the feedback principle overrides the usual velocity relations in ordinary laminar flow is demonstrated. With flow rate as an additional variable, certain limitations inherent in requriements of gravitational stability of static density-gradient columns (e. g., in solution composition, sample capacity, and heat dissipation) are removed. Since complete analysis of such density stability must await advances in basic theory of multiple-transport processes in solution, the importance of the experimental approach is emphasized.

Migration principles, especially for sedimentation and electrophoresis are classified as rate, or equilibrium, and the known and unknown elements of several examined. A simplified Stokes-type treatment is sufficient for semiquantitative description of individual cell sedimentation under 1 g, including calculation of resolution and separation time. A kind of experimental cell behavior called

For such investigations, speed may be much more than just a convenience; it may lead to qualitatively different results. Without knowing exactly what changes are taking place after removing biological material from its natural environment, the investigator can often be quite sure that irreversible processes are in fact occurring. He may be further frustrated upon ascertaining that his own procedures are at least partly responsible for these changes and yet he may be forced to settle for such altered material as the best available. If, however, separation procedures and subsequent studies can be completed in a few minutes under mild conditions, then irreversible processes occurring with a longer time scale (e. g., hours or days) may not seriously interfere.

The particular role in such work of the stable-flow free boundary (STAFLO) method in permitting rapid, continuous, high-resolution steady-state migration, with separate collection of components, in free solution yet inherently stabilized against convection, has already been discussed.[1] Although the first results reported were achieved with use of an electric field (i. e. electrophoretic), possible use of other fields was suggested.[6] The purpose of this paper is to discuss in more detail some theoretical and experimental aspects particularly pertinent to work with living cells, and especially the use of a 1 g gravitational force field (sedimentation).

II. APPARATUS

A. Flow-Cell and Collection System

The apparatus for cell studies (designated No. 2) is basically that used for the molecular interaction study.[7] An overall schematic drawing of the essential components of the whole apparatus is given in Fig. 1, and the flow-cell shown in more detail in Fig. 2. The main migration chamber of the flow-cell is 30 cm long, 3 cm high, and 0.7 cm wide. Thus, each of the symmetrical 12 inlet-outlet combinations feeds in and exits, respectively, a 0.25×0.7-cm cross-sectional area, and therefore services a liquid volume of 5.25 ml (1/12 of the total 63 ml migration-chamber volume). This, then, amounts to the minimum solution volume that could establish steady-state flow conditions, given these particular dimensions. Though for ease in machining, the inlet-outlet end pieces have sometimes been made of epoxy plastic, for maximum visibility the entire flow-cell is conveniently made of Lucite.

Difficulties often encountered in sealing liquid-flow apparatus assembled from several parts have been obviated by use of the simple tongue-and-groove construction, with the cellophane (dialysis tubing) semipermeable membrane acting as a gasket between the electrode compartments and migration chamber. The main purpose of the membranes is to serve as isolation barriers, of high hydrodynamic yet low electrical resistance, for the migration chamber. To insure against capillary leaks out the ends (along the tongue-and-groove channels), 0.5-in. strips of sheet paraffin are usually placed at the ends, above and below the membrane. The first model constructed was held together by a large number of stainless steel bolts. This complicated the assembly (clearance holes in the membranes had to be made and accurately held in position to prevent the membranes' being caught by the bolts during tightening) and made disassembly of the apparatus for cleaning or changing the membrane somewhat tedious. The present system of holding the assembled flow-cell is entirely satisfactory. The supporting stand has a hinged support point to allow easy tilting of the apparatus for flushing out air bubbles, and is fitted with three leveling screws for fine adjustment. Assembly is accomplished by carefully squeezing the three parts of the flow-cell together in a vise, then placing it in the stand and clamping it. There is usually enough friction to hold the parts sealed together, even without the clamps.

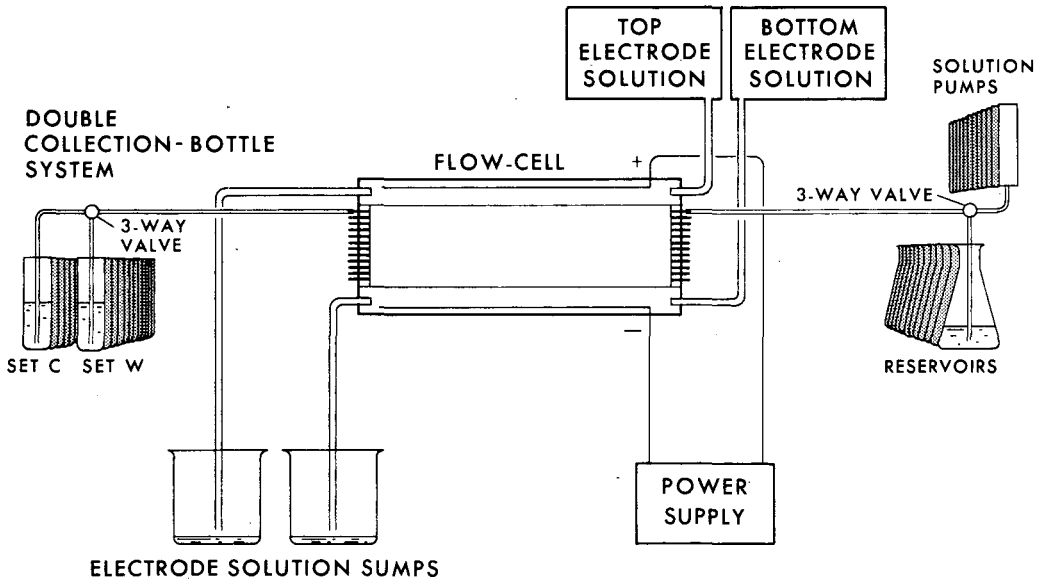

Fig. 1. Stable-flow free boundary (STAFLO) apparatus.

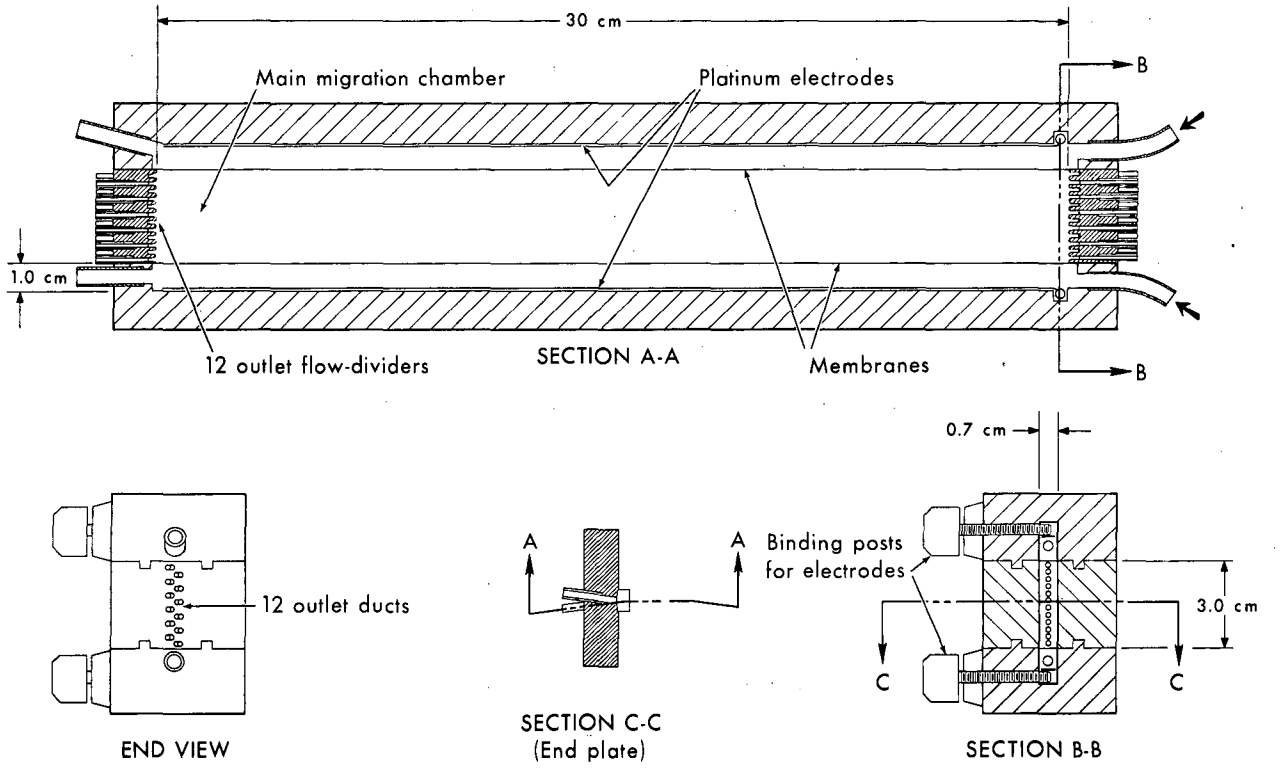

Fig. 2. STAFLO flow cell No. 2.

The membrane is commonly a single thickness of dialysis tubing which is thoroughly soaked before installation and not allowed to dry out subsequently. For free-flow sedimentation only, the membrane and electrode compartments are not necessary, but for convenience they are generally left in place so that an electric field can be applied whenever desired. For certain analytical studies with electric field, the physical and electrical properties of the membrane can affect the experimental results, so attention should then be paid to these properties. Conceivably, for future high-current density applications, the simple dialysis membrane may profitably be replaced with a more sophisticated ion-exchange membrane.

The collection system should be considered with the flow-cell, for the hydrodynamic unity of the 12 collection fractions with the migration chamber is a principal feature responsible for stable flow. Either of the duplicate sets of 12 collection containers can be connected to the flow-cell by the 3-way valves (Fig. 1). Recently, it has been found most convenient and economical to employ as collection containers the barrels of disposable plastic syringes. The tips are sealed, and holes are drilled in the base of a separate stand to receive the tips. Rapid suction emptying of set W (not shown in Fig. 1) has proved more convenient than using much larger receptacles. Although more than 12 collection fractions can be employed and may eventually be desirable for certain purposes, the added inconvenience of handling additional fractions has not yet been justified.

Polyethylene tubing of i.d. 0.062 in., to fit the No. 16 inlet-outlet needles, is preferred over the equivalent Tygon tubing if spectra are to be run, as Tygon exudes for a long time strongly ultraviolet-absorbing materials. An important variation, for work with living cells, is the substitution of a polyethylene tube i.d. 0.015 in. for the cell feed-in. In this smaller-diameter tube, the linear flow rate at the usual volume flow rates is sufficiently fast to prevent sedimentation and piling up of the cells, which can otherwise interfere with orderly feeding of samples into the migration chamber.

B. Pumping and Electrical Systems

A convenient 12-channel pumping system continues to be a rack of 12 identical, ganged plastic syringes (commonly 20 to 50 ml each) driven in concert by a synchronous motor with a Zero-Max variable-speed transmission.[8] An auxiliary high-speed motor is useful for filling the syringes and for fast flushing operations. This is by no means the only feasible pumping system, and other

simpler ones have been successfully employed. It does provide positive-drive smooth pumping, however. The syringes are filled in place from individual reservoirs connected via three-way valves (Fig. 1). The cell-sample syringe is stirred magnetically.

For independent, electrode compartment fluid flow, constant-head capillary-controlled gravity feed is employed.[9] To monitor these flow rates, simple spherical float flow meters are very useful.[10]

For electrophoretic operation with low current (e.g., < 40 mA) a Heathkit voltage-regulated power supply is quite suitable.[11] For high-conductivity solution experiments, however, where regulation at low voltage and higher current is required, the Heathkit must be replaced by an appropriately designed power source. The platinum foil electrodes can be cemented in place, or held physically by being extended sidewise into thin slots. Though the electrode solutions exit into beakers and are usually discarded, they can be recycled if desired.

(For a photograph of the overall apparatus, see Fig. 5 in Ref. 1.)

III. FLOW STABILITY

A. General

The sine qua non of a high-resolution continuous free-solution analytical or separation process is stability of flow. If the constant total flow supplied distributes itself differently amongst the outlets at different instants of time, then complete multicomponent separations are difficult or impossible. Since time-varying flow velocities at the outlets, because of the nature of a viscous fluid, will be associated with upstream "waviness" or other disturbance of the flow pattern, high-resolution analytical studies would also be ruled out. A closely related aspect, implied in overall flow stability, is absence of internal convection during the differential migration of the various species. Tiselius achieved this for the U-tube apparatus by careful mounting and by thermostating near the temperature of maximum solution density.[12] As has been repeatedly noted in the literature, however, prior to the STAFLO method[1,6] the main aspect (i.e., the stability of flowing streams) had not been solved.[13,14,15]

The first attempt at true free-flow electrophoretic migration was by Philpot.[16] His idea for flow stability is indicated in the title of his paper, "Thin Layers in Electrophoretic Separation," i.e., use of stable density gradients, employing solutions with glycerol, ethyl alcohol, and methyl alcohol. Though he specifically intended the method for use with proteins, no results were reported and, in fact, he expressed doubt that this would even be possible. His problems with flow and his generally pessimistic conclusions (including those from mathematical analysis of such factors as sample dilution and heat production) were very likely important in directing subsequent work into the multifold supporting-medium approaches using starch, paper, glass beads, etc. Aside from continuing free solution work on electroconvection and electrodecantation (which require convection) a number of years elapsed before appearance of significant new approaches of this kind. Although these have employed certain anticonvection measures (such as use of membranes, additional restrictions on flow, internal thickening agents) they are much closer to unrestricted free-solution methods. There are very good recent reviews on the subject,[17,18,19] and only a few highlights are mentioned here--particularly, those pertinent to flow and stability.

By introducing a series of channels separated by filter paper, Schumacher and Flühler confined flow and reduced convection to a single channel, but, of course, were restricted to use of small migrating species.[20] Bier, by counter-

current flow and membrane filtration,[21] separates an isoelectrically immobilized protein from the mobile components in a mixture of proteins or even in whole blood.[19]

In reports on their vertical electrophoretic apparatus, Dobry and Finn refer to the difficulties of establishing and maintaining steady flow and to the unsolved problems in this regard.[14] Their sample is fed in at a lower velocity than that of the adjacent solutions ("hypokinetic conditions"), and to reduce internal convection they add to solutions a high-viscosity polymer (e. g., dextran). With their minimum usable flow rates, even with a 5-foot column, the retention time in the column is only 3 to 4 minutes, which apparently precludes protein separations by the method described.

Electrophoresis has recently been conducted in capillary-thickness flowing layers. Barrolier's method using very thin, flat layers[22] has particularly been developed by Hannig[23] who reports separation of human and rabbit erythrocytes),[23] and also used by Wolfgang[24] (in whose method the sample is in contact with paper for a short time). Kolin employed an annular layer and demonstrated, on a microscale, interesting spiral migration of dyes in an electromagnetic field.[25] Whether this will work with biological samples or whether it can be scaled up to significant flow rates or sample concentrations remains to be seen. The overall geometry dictated by the capillary-thickness requirement introduces certain problems and limitations not unlike those found with the previous supporting-medium approaches, e. g., in range of possible flow rates, in high voltage requirements in power requirements and heat dissipation, and (for cell work) the problem of the cells' hitting the nearby surface.

In none of these approaches is there intrinsically stable bulk solution flow. As Raymond remarked,[13] "Experience with apparatus where separation depends on a constant and continuous flow of solution through the apparatus has demonstrated that many difficulties are encountered in adjusting and maintaining the proper rates of flow." Svensson also has remarked recently, in referring to Philpot's work, "...problems connected with the flowing solutions were, however, very tough and not solved."[15] The solution of the basic flow problem, by the STAFLO method, is the subject of the remainder of Sec. III.

The nature and degree of flow stability in the larger sense, for the STAFLO method, is indicated by the pattern of Fig. 3, and by the fact of equal volume flow of liquid into each collection bottle per unit time during this flow experiment. This photograph of the steady-state condition in the absence of any significant external force field (other than 1 g) was taken under the following conditions: flow of

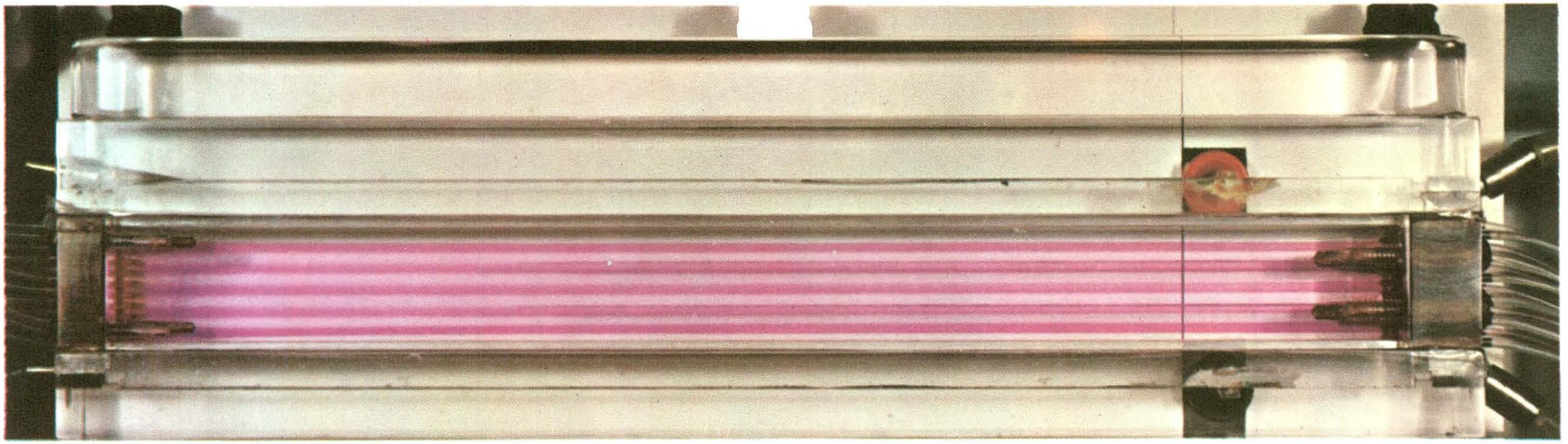

Fig. 3. Steady-state flow pattern in the absence of electrical field.

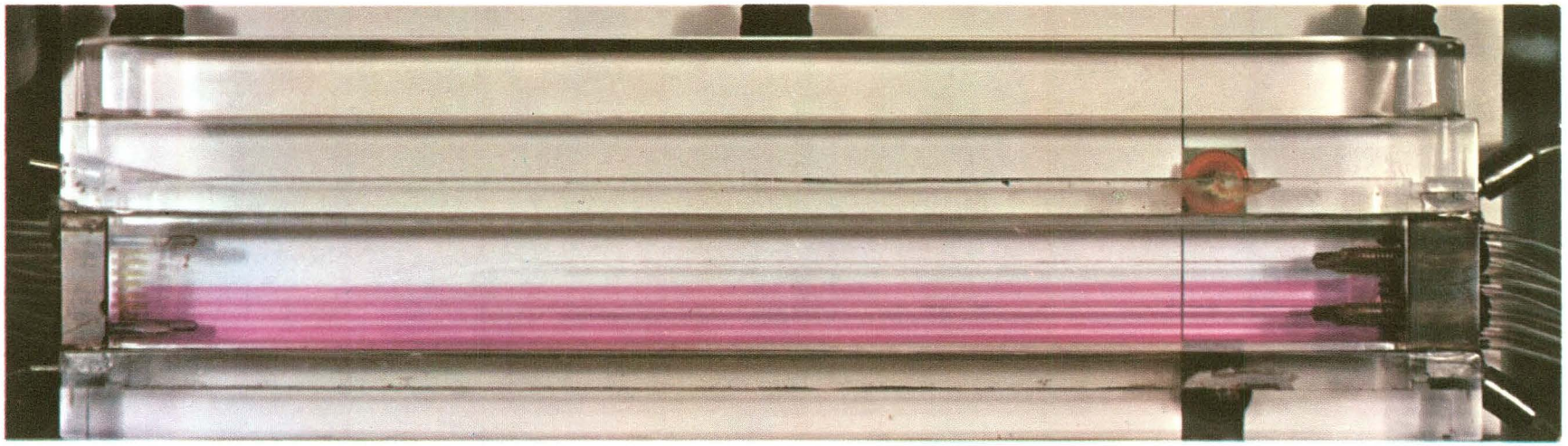

Fig. 7. Pre-steady-state flow pattern in the absence of electrical field.

1.35 cc/min/inlet, 16.2 cc/min overall; linear velocity 7.7 cm/min; sucrose gradient, top to bottom; 0 to 7.5%; dye added to Nos. 3, 5, 7, 9, 11. No thermostating or shock mounting was involved. Each entering stream is exiting essentially completely from only its corresponding outlet after the 3.9-min passage through the flow-cell. The principles responsible for this stability and for "flow stability" as used in the general sense in this paper, are: (a) self-balancing hydrodynamic feedback; (b) laminar flow;* (c) density-gradient stability. Previous approaches, including those specifically noted above, have utilized (b) or (c) [or even (b) combined with (c)], but none had all three, nor, indeed, (a) alone. We will now examine each of these points in some detail.**

B. Self-Balancing Hydrodynamic Feedback

This follows from basic hydrostatic and hydrodynamic principles. It is instructuve to examine these more closely, since the geometry of the cell-plus-collection system at first glance may tend to obscure some of the simple physical relationships involved.†

1. Hydrostatic balance

Consider first the hydrostatic circuit of the flow-cell in Fig. 4a, completely filled with liquid, at equilibrium at some instant in time. The inlet syringe pumps are not specifically shown, since they can be considered part of the same closed system with the cell; for simplicity, only two collection bottles are considered. Unless otherwise specified, we will hereafter assume vertical collection containers of uniform cross section, as pictured. This circuit is entirely equivalent to the simple siphon circuit of Fig. 4b. With uniform liquid density throughout and with atmospheric pressure applying equally to both liquid surfaces, the equilibrium condition is, of course,[26]

$$h - \ell_1 = h - \ell_2; \text{ i.e., } \ell_1 = \ell_2. \tag{1}$$

---

* "Laminar flow" is here used in the broad sense, not restricted to usual velocity relations; see discussion in Sec. III. C.

** To aid the subsequent reading, it will be helpful to refer to the short list, Definitions and Basic Concepts, in the appendix.

† The geometry also plays a theoretical role in the migration and separation of components as discussed in Sec. IV.

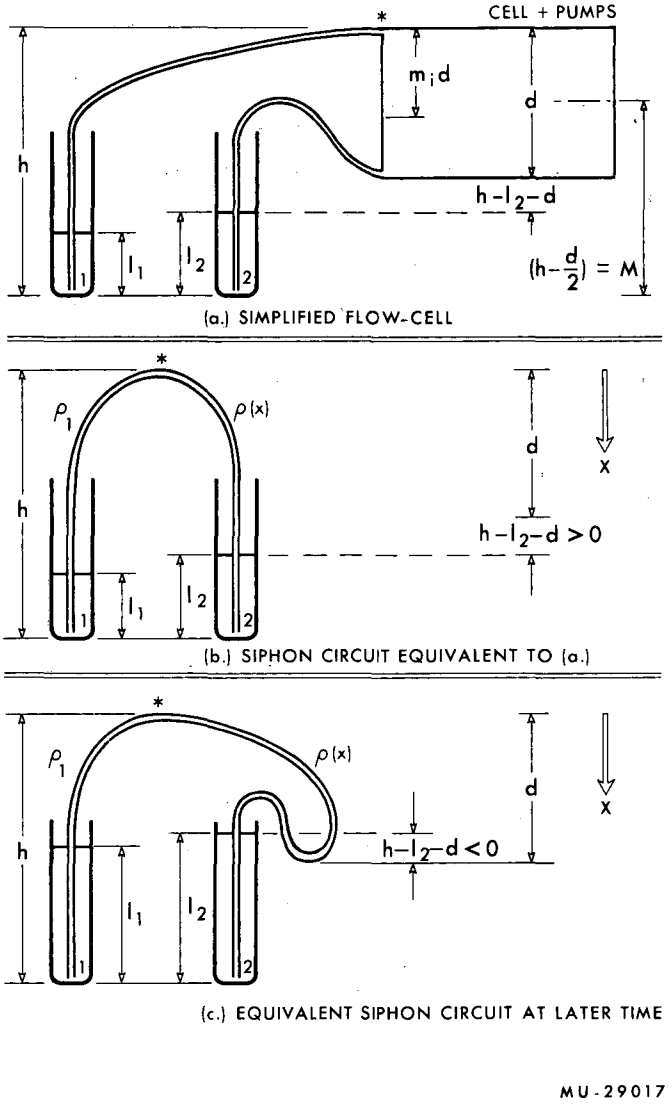

Fig. 4. Equivalent hydrostatic circuits of simplified flow-cell and siphon.

(Note that the depth of the tip of the siphon below the liquid surface does not enter into the equation.)

When the cell contains solutions with density increasing from top to bottom, the mass of the column of liquid in the right-hand arm of the siphon exceeds that in the left arm. For the static condition of no flow of any kind we can write a pressure balance at the point marked by an asterisk(*).

$$(\text{atmos}) - \rho_1 g(h-\ell_1) = (\text{atmos}) - g \int_0^{h-\ell_2} \rho(x)\,dx. \qquad (2)$$

The coordinate x is measured positively downward from the asterisk; ρ_1 and $\rho(x)$ are the solution densities in the left and right arms, respectively, and ℓ_1, ℓ_2, and h are the heights indicated in Fig. 4b. Note that $\rho(x)$ is no longer a single-valued function of x when the liquid level ℓ_2 has risen above the height of the bottom of the flow-cell, i.e., when $(h-\ell_2 - d) < 0$; therefore, to be general, we must draw the equivalent siphon circuit as in Fig. 4c rather than Fig. 4b. Also, assuming $\rho(x)$ inside the cell to be constant in time, the part of the siphon in Fig. 4c outside the cell between x=d and $x=h-\ell_2$ will always contain liquid of density ρ_2, whether the siphon has a reverse loop as in Fig. 4c, or not, as in Fig. 4b. Consequently, we can simplify and rewrite our basic hydrostatic Eq. (2) as

$$\rho_1 (h - \ell_1) = \int_0^d \rho(x)\,dx + \rho_2 (h - \ell_2 - d), \qquad (3)$$

with d, the cell height, indicated in Fig. 4.
As a representative $\rho(x)$ consider the linear function*

$$\rho = \left(\frac{\rho_2 - \rho_1}{d}\right) x + \rho_1 , \qquad \text{with } \rho_2 > \rho_1 . \qquad (4)$$

Substituting Eq. (4) into (3) and integrating, we find

$$\rho_1 (h - \ell_1) = \rho_2 (h - \ell_2) - \left(\frac{\rho_2 - \rho_1}{2}\right) d. \qquad (5)$$

---

*This density function is sufficiently general for the purpose of the present illustration, and by proper choice of variables can be closely approached. $\rho(x)$ may sometimes have some time dependence, but this is not usually critical to the argument which follows.

Alternatively, we can write

$$\frac{\ell_2}{\ell_1} = \frac{M}{\ell_1}\left(1 - \frac{\rho_1}{\rho_2}\right) + \frac{\rho_1}{\rho_2} \quad , \tag{6}$$

where $M = (h - d/2)$ depends only on dimensions of the apparatus.

(Similar, but not identical, equations will apply for any pair among the usual 12 collection containers.)

Equation (6) is the basic equation of instantaneous hydrostatic balance for the system, with a linear gradient and with any given ρ_1, ρ_2, and M. If a fluctuation should cause a momentary deviation of ℓ_2/ℓ_1 from that consistent with Eq. (6), an appropriate restoring force would operate to correct the imbalance, hence the self-balancing feedback property. A static equilibrium condition of particular interest is that of $\ell_1 = \ell_2$; it is often closely approximated during flow experiments in the laboratory, it coincides with the intuitive idea of a simple siphon, and it stands in special relation to the normal position of the steady-state pattern, as discussed later. If this particular condition held at each succeeding instant in time during the flow process, we would be assured of equal volume outflow per unit time per collection tube. Thus it is a sufficient condition for equal outflow rates, though not a necessary one (as will be seen later). Aside from the limiting case of $\rho_1 = \rho_2$, from Eq. (6) we will also have this condition $\ell_1 = \ell_2$ for all density gradients, if we have

$$\ell_1 = M \quad (= \ell_2), \tag{7}$$

i.e., when the collection bottle levels have risen to the halfway height in the flow-cell (see Fig. 4a).

To illustrate the equilibrium-determined deviation of ℓ_2/ℓ_1 from unity for different density conditions, let us evaluate from Eq. (6) the parameters ℓ_2/ℓ_1, ℓ_1, and ℓ_2 as functions of M/ℓ_1, which generally changes during the flow process. Some results are given in Table I, for 20° C, assuming pure water in No. 1 and different sucrose solutions in No. 2, having the compositions indicated. (The ℓ_1 and ℓ_2 are expressed as percentages of the height M.) As expected, the deviation of ℓ_2/ℓ_1 from unity is seen to be small when $\rho_1/\rho_2 \approx 1$ or when $M/\ell_1 \approx 1$. For higher densities and with M/ℓ_1 far removed from 1.00, the deviation appears large. Thus, for 50% sucrose in No. 2, when $\ell_1 = 0.0333M$, ℓ_2 is 6.45 times ℓ_1. Later, with $\ell_1 = 0.10M$, ℓ_2 is 2.69 times ℓ_1. Before pursuing this further, recall that these calculations are analogous to those for the extreme tubes of a set of 12. Level differences between receptacles for adjacent streams, having average density differences only 1/11 of those shown, will be considerably smaller.

Table I. Evaluation of parameters from Eq. (6).

		Weight % sucrose in No. 2									
		0		5		10.5		33.1		50	
		ρ_1/ρ_2									
		1.000		0.980		0.960		0.874		0.812	
M/ℓ_1	ℓ_1*	ℓ_2/ℓ_1	ℓ_2*	ℓ_2/ℓ_1	ℓ_2*	ℓ_2/ℓ_1	ℓ_2*	ℓ_2/ℓ_1	ℓ_2*	ℓ_2/ℓ_1	ℓ_2*
30	3.33	1.00	3.33	1.58	5.27	2.16	7.2	4.65	15.5	6.45	21.5
10	10.0	1.00	10.0	1.18	11.83	1.36	13.6	2.13	21.3	2.69	26.9
3	33.3	1.00	33.3	1.04	34.7	1.08	36.0	1.25	41.7	1.38	45.9
1.5	66.7	1.00	66.7	1.01	67.3	1.02	68.0	1.06	70.9	1.09	72.9
1.0	100.0	1.00	100.0	1.00	100.0	1.00	100.0	1.00	100.0	1.00	100.0
0.6	166.7	1.00	166.7	0.99	165.3	0.98	164.0	0.95	158.3	0.92	154.1

*Expressed as a percentage of M.

For colorless solutions, the receptacle levels are the most obvious observables for monitoring the course of a flow experiment, and Table I gives us the theoretical hydrostatic values for comparison. However, a more important aspect of the levels is their relation to volume flow and to the flow pattern. We now examine the implication of Eq. (6) for (a) differences in integrated volume outflows over finite periods of time, (b) simple displacement of the steady-state pattern from its normal geometrical position, and (c) possible drift, or a non-steady-state component of pattern. To consider these points it is instructive to plot in Fig. 5 the linear functions $\ell_1^* (=\ell_1/M\times 100)$ and $\ell_2^* (=\ell_2/M\times 100)$ vs $\frac{\ell_1^* + \ell_2^*}{2}$, for the two cases of 50% sucrose in No. 2 and 5% sucrose in No. 2 (data calculated from Table I). The quantity ℓ_i^* is proportional to V_i, the volume in the ith collection bottle, and $\frac{\ell_1 + \ell_2}{2M}$ is proportional to total volume flowed. With incompressible fluids and a rigid flow-cell-plus-pumping system, the constant total inflow rate assures (the same) constant total outflow rate. Thus, for a specified flow and specified collection bottle size, Fig. 5 is equivalent to a plot of V_i vs t.*

Considering point (a) first; from Fig. 5 we can readily see, for equilibrium conditions with any total volume flowed, the degree to which V_2 exceeds V_1. Thus, with a 0 to 50% sucrose gradient, if $\ell_1 + \ell_2$ varies between 50% and 160% of 2M, V_1 and V_2 will always differ by less than 22%. (If this same reasoning applied directly to all 12 tubes with the same overall gradient, adjacent equilibrium volume differences would always be less than 2% under the circumstances, but this is not exactly so, as discussed below.)

The slopes of the lines in Fig. 5 are directly proportional to the respective outflow rates Q_1^{out} and Q_2^{out}. Note particularly that, although V_2 is always somewhat greater than V_1, this must result from an initial condition. During the flow experiment, Q_2^{out} is constant and always less than Q_1^{out}. This can also be seen directly from Eq. (6), from which we can calculate

$$Q_2^{out}/Q_1^{out} = \frac{d\ell_2}{dt} \Big/ \frac{d\ell_1}{dt} = \rho_1/\rho_2 \ (<1). \qquad (8)$$

This situation is entirely consistent with a steady-state pattern, albeit a displaced one. With incompressible fluids and the closed, rigid nature of the flow-cell-plus-pumping system we can quickly estimate, from Eq. (8) or Fig. 5, the

*Until otherwise stated, a stronger condition is also implicit in this discussion, namely, that the outflow rate of each solution i equals its inflow rate.

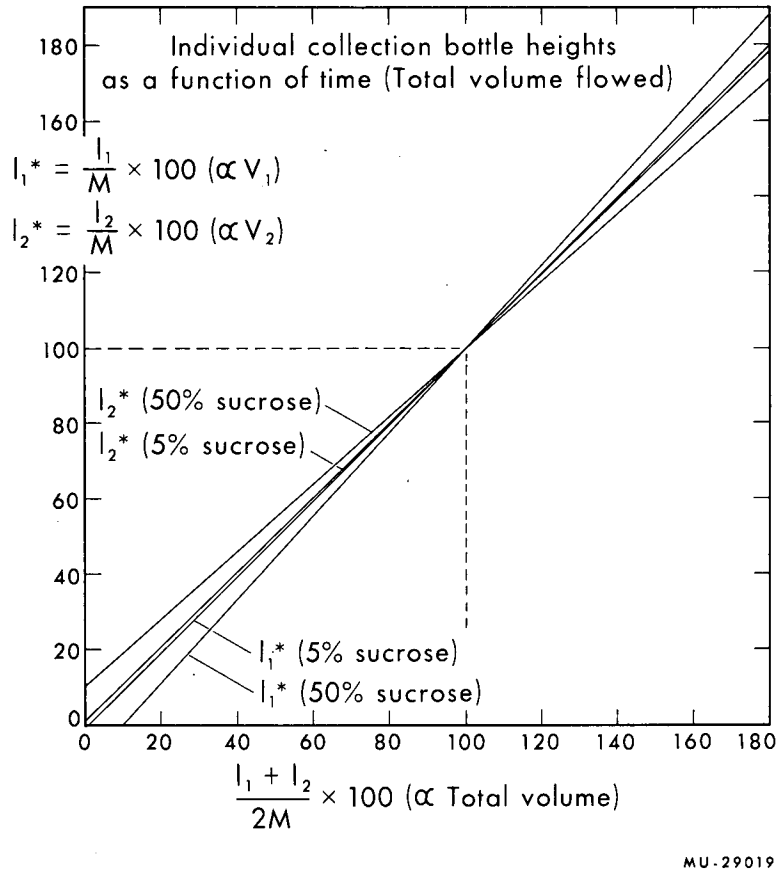

Fig. 5. Individual collection-bottle heights as a function of time (total volume flowed).

steady-state displacement for the different density gradients. We have, for example

	0 to 50% sucrose	0 to 5% sucrose
Q_2^{out} / Q_1^{out}	0.812	0.98
Corresponding average percentage difference between outflow rates Q_2^{out} and Q_1^{out}	~ 21%	~ 2%
Corresponding Q_1^{out} excess and Q_2^{out} deficit compared with Q_1^{in} and Q_2^{in} respectively	~ 10.4%	~ 1%
Corresponding upward displacement of the steady-state flow pattern	~ 10.4%	~ 1%

A flow-pattern displacement, even a fairly large one, is of little consequence for many purposes as long as it represents a steady-state condition. For some purposes, particularly analytical, a normal pattern position is desirable, however. A possible mechanical means of inducing and maintaining the normal pattern position follows from the earlier discussion and Eq. (6). If we now permit movement of the collection-system platform--i.e., variation in M--the time derivative of (6) has the form

$$\frac{d\ell_2}{dt} = \left(1 - \frac{\rho_1}{\rho_2}\right) \frac{dM}{dt} + \frac{\rho_1}{\rho_2} \frac{d\ell_1}{dt} \quad . \tag{9}$$

By selecting the rate of movement dM/dt equal to $d\ell_1/dt$, Eq. (9) is reduced to

$$d\ell_2/dt = d\ell_1/dt, \quad \text{or} \quad Q_2^{out} = Q_1^{out}. \tag{10}$$

If the platform movement is started just when the $\ell_2/\ell_1 = 1$, this ratio (hence equal outflows) will be subsequently maintained, in accordance with Eqs. (7) and (10).

Discussion of the remaining aspect of Eq. (6), i.e., pattern drift, now becomes pertinent. The inequality (8) corresponds to a displaced pattern and the equality (10) to a normal pattern, in the steady state; thus, by starting this platform movement, we maintain $\ell_2/\ell_1 = 1$ but cause a shift of pattern to the normal. The time required to reach the normal steady-state position depends on the flow rates and relative volumes of collection containers and flow-cell. (This shift requires the temporary condition $Q_{soln\ i}^{out} \neq Q_{soln\ i}^{in}$ as discussed in Sec. III. B. 3.)

Since steady-state equal outflows imply a normal pattern position, it is appropriate here to consider a more general necessary condition for equal outflows, to which earlier reference was made. Integration of Eq. (10) gives us this condition, namely

$$\ell_2 - \ell_1 = \text{constant}. \tag{11}$$

The previous condition (7) is the special case with the constant = zero, which allows the ratio of ℓ_2 over ℓ_1 (unity), as well as the difference between ℓ_2 and ℓ_1, to be maintained constant. However, from Eq. (11), 1 is the only such constant ratio compatible with equal outflows. Starting with any other condition $\ell_2/\ell_1 \neq 1$, if the platform were moved as before, the ratio would gradually change, approaching 1 as a limit. The constant difference (11) would always remain, and the normal flow pattern (as soon as attained) would also remain. We can evaluate this difference in terms of the other parameters of the system, from Eq. (6):

$$\ell_2 - \ell_1 = (M - \ell_1)\left(1 - \frac{\rho_1}{\rho_2}\right). \tag{12}$$

If the difference is to remain constant, we see again directly that M must be kept equal to ℓ_1.

Independent control of the change of ℓ's per unit volume flowing is available by suitable choice of dimensions for the collection containers. Thus by use of inverted cones, or right circular cylinders of larger diameter, the ℓ's can be maintained approximately constant for substantial times. This is not at all the same as the exact mathematical condition (11) brought about by platform movement, and does not affect the steady-state position of the flow pattern as did conditions (10) and (11).*

Additional aspects of flow-pattern position and drift are considered in Sec. III. B. 2 and Sec. III. B. 3.

Arbitrary number of collection fractions. The extension of these arguments from two to an arbitrary number of collection fractions is not trivial. Returning to the basic hydrostatic circuit of Fig. 4,

---

* Long-time collection with small containers is simply accomplished by timely switching of the three-way valves (Fig. 1) from one set to the other, then emptying the full set. Care must be taken only that each set is leveled before connecting it to the flow-cell.

assume "i" inlet-outlet combinations and consider an arbitrary fraction with level ℓ_i, whose outlet occurs at the position $x = m_i d$. We can then rewrite Eq. (3) as

$$\rho_1 (h - \ell_1) = \int_0^{m_i d} \rho(x)dx + \rho_i (h - \ell_i - m_i d), \text{ with } 0 < m_i < 1. \quad (13)$$

Rewriting the density function (4) in the form $\rho(x) = (\frac{\rho_i - \rho_1}{m_i d}) x + \rho_1$, we can integrate (13) and obtain analogues of Eqs. (5) and (6), of which we need only to consider the latter:

$$\frac{\ell_i}{\ell_1} = \frac{M_i}{\ell_1} (1 - \frac{\rho_1}{\rho_i}) + \frac{\rho_1}{\rho_i}, \quad \text{with} \quad (14)$$

$$M_i = (h - \frac{m_i d}{2}) = \frac{(h - \frac{m_i d}{2})}{(h - \frac{d}{2})} M. \quad (15)$$

The new elements here are that M_i is different for each fraction and that these differences themselves depend on the apparatus parameters h and d. The special static equilibrium condition of $\ell_1 = \ell_i$ now follows from

$$\ell_1 = M_i. \quad (16)$$

Unlike the situation represented by Eq. (7), here the M_i are all different, so that the levels ℓ_i cannot all be equal at precisely the same instant.

To determine the effect of this on the levels of the collection bottles and on the steady-state pattern distortion, one must recalculate Table I and Fig. 5 according to Eq. (14) for all fractions. Since each ℓ_i remains a linear function of ℓ_1, each ℓ_i is also a linear function of $\sum_1^n \ell_i$, with n the total number of fractions. Plots of ℓ_i, using $\sum_{i=1}^{12} \frac{\ell_i}{12M}$ as abscissa, strongly resemble Fig. 5, though the lines do not all intersect exactly at the 100% coordinates. From Eq. (15) it is seen that for $h >> \frac{d}{2}$, $M_i \approx M$, so a suitable choice of h and d allows us to recover the universal equal-level condition analogous to (7), to a very good approximation. If we choose d=3 cm, and h=5 cm (common for apparatus No. 2, Figs. 1 and 2) and choose the extreme sucrose gradient of 0 to 50% (using values of $m_i = \frac{12}{12}, \frac{11}{12}, \cdots$ etc.) such calculations reveal that for $\ell_1 = M$ $(= M_{12})$ the maximum deviation of any ℓ_i from ℓ_1 is 2%; the average deviation

between ℓ_i of adjacent tubes is ≈ 0.4%. For a more recent apparatus No. 6, with h = 7 cm and d = 1.5 cm, a similar calculation shows the maximum deviation to be 0.6%, and the average adjacent deviation is ≈ 0.1%.

In the region of small ℓ_i, the curves for ℓ_1 and ℓ_{12} for both apparatus are very similar to the 50% sucrose curves of Fig. 5. Since they do not all intersect at the 100% coordinates, however, the relative order at any time $\ell_1 < \ell_2 < \cdots < \ell_{12}$ only holds exactly until the first two lines ℓ_i cross over as determined graphically, or as determined from solving Eq. (14) for the conditions $\ell_i = \ell_k$. In the present example, this "lowest crossover point" is for $\ell_{12} = \ell_{11}$, and occurs at an abscissa of about 60%; for apparatus No. 6 it occurs at an abscissa of about 90%. At the 50% abscissa, for apparatus No. 2, the values of ℓ_1/M and ℓ_2/M of 0.44 and 0.55 in Fig. 5 become values (for ℓ_1/M and ℓ_{12}/M) of 0.43 and 0.54, with all the other ℓ_i included between these two. Thus, even with this relatively "unfavorable" h and d, and an extreme sucrose gradient, the change is small. The constant slopes of the lines ℓ_i/M vs $\sum_1^{12} \ell_i/12M$ satisfy the expression

$$\frac{d\ell_i}{dt} \Big/ \frac{d\ell_1}{dt} = Q_i^{out}/Q_1^{out} = \rho_1/\rho_i \quad (< 1). \tag{17}$$

Equation (17) follows from Eq. (14) exactly as did Eq. (8) from Eq. (6). Thus the relation $Q_{12}^{out} < Q_{11}^{out} < \cdots < Q_1^{out}$ holds, the steady-state nature of the flow-pattern is assured, and the displacement can be calculated as before. Of course, the most significant feature of pattern displacement is its local aspect, i. e., the position of each local flowing layer relative to its corresponding outlet. With the stated sucrose gradient spread over 12 tubes rather than just two, density differences between adjacent streams are much smaller. Hence, local displacements are correspondingly diminished, commonly to negligible values.

In sum, then, with a little care, the hydrostatic arguments for level-flow stability, including pattern position and drift, based on two-fraction collection, can be applied to the n-fraction case. The more lengthy complete calculations for many fractions can be carried out whenever desired. Additional elements, such as the effects of different initial ℓ's, might properly be included in this general hydrostatic analysis of Sec. III. B. 1. They will not by pursued further at this time, however, for reasons apparent from the discussion that follows.

2. Hydrodynamic Considerations

The ideal result of a hydrodynamic analysis of STAFLO behavior would be the calculation of the individual outflow velocities Q_i^{out} from the first principles of fluid mechanics, where we take into account fluid velocity, viscosity, and other flow resistance factors inherent in the experimental setup. This is a very complicated undertaking. Even if we neglect the important frictional factors, density gradients, etc., an exact calculation of this kind appears impossible (see the discussion on laminar flow, Sec. III. C.). Furthermore, for a realistic calculation, the results would be highly dependent upon particular apparatus configurations and experimental conditions. It will be sufficient at this juncture to examine the qualitative effect of the flow resistance factors on the steady-state condition and the flow-pattern position, and to interpret the general STAFLO experimental observations in these terms. The result is to supplement but not supplant the previous hydrostatic line of reasoning.

The previous hydrostatic calculations pertain to the limiting conditions of slow flow and low hydrodynamic resistance, i. e., low solution viscosities and/or short lengths of large diameter tubing. A particular result was that below the lowest "cross-over point" (or, if we have appropriately chosen the h, d, and ρ_i, for $M/\ell_i > \approx 1$), equilibrium hydrostatics implies that levels of denser liquids will be higher than levels of the less dense; e. g., $\ell_{i+1} > \ell_i$. In actual fact, with the ranges of operating parameters customarily employed with the STAFLO method, under such circumstances when a difference exists the contrary relationship is experimentally observed, i. e., $\ell_{i+1}/\ell_i < 1$. However, the qualitative outflow relations--e. g., the inequality following Eq. (17)--remain. No inherent long-term instability or pattern drift has been observed. The system is still characterized experimentally by a stable steady state (but a different one). This has been true for runs lasting through 8 throughput volumes (e. g., > 4 hrs.) with sucrose gradients of 0 to 40% and with those minimal flow rates found to be useful (e. g., 30 to 60 min transit time through a 30-cm long apparatus). The movement of colored solutions relative to the fixed inputs and outputs is easy to see and to record photographically to verify this point.*

* One can also test rapidly the stability of relative levels in different collection tubes during the flow process. A small increment of liquid is added directly to, or subtracted from, any one (or more) of the tubes thus creating an artificial difference between its level and that of the others. If all such differences are seen to be self-correcting, then the system is adjudged stable in this sense.

Reasons for this behavior can be found in the viscous nature of the solutions and the experimental parameters employed. The densest (bottom) solutions used with the steepest gradients (for which the "ℓ" inequalities should be most evident) have had higher viscosities and, therefore, significantly higher resistance to flow. All solutions are forced into the flow-cell at the same constant rate, but the more viscous ones tend to exit more slowly at the start, resulting in the relation $\ell_{i+1} < \ell_i$. This leads initially to a relative build-up of denser solutions inside the flow-cell. Thus, as in the purely static case there results an upward shift in the flow pattern, but for a different reason. Experimental observation is that the flows balance shortly, and a steady state is established with the upward-displaced flow-pattern. The most obvious reasons for this are:

(a) This movement of liquid tends to be self-correcting as the ℓ-relations become increasingly contrary to the hydrostatic equilibrium.

(b) The relative buildup of denser solution in the flow-cell increases the pressure at the lower outlets, tending to increase their otherwise reduced flow.

(c) An inherent, self-limiting feature of the viscous effect also exists: As the pattern moves upward, expanding at the bottom, compressing at the top, the total outflow resistance for the most viscous solutions decreases, and outflow resistance for the least viscous increases.

The principal pertinent flow-resistance features of the apparatus are (see Figs. 1 and 2): (a) the existing orifices: stainless hypodermic needles, No. 16 (i.d. = 0.045 in.) or No. 19 (i.d. = 0.026 in.) and 0.38 to 0.5 in. long; (b) the tubing from these outlets to the valves and collection bottles: 7 in. of 0.062 in. i.d. plus 5 in. of 0.070 i.d., connected by appropriate small metal valves and adapters, commonly used for medical purposes.[27] Work with other forms of the apparatus shows these values not to be especially critical.

3. Combined Viewpoint

The title of Section III. B, "Self-Balancing Hydrodynamic Feedback" is meant to imply the combined hydrostatic, hydrodynamic interplay and effect on flow stability. Although the hydrostatic principles discussed in such detail above are not necessarily the primary factors determining the flows, nevertheless, a thorough understanding of them is important for reasons which may be summarized as follows:

(a) For a large number of useful experiments, including most of those performed to date, they provide a satisfactory description of flow behavior.

(b) They are the primary flow-determining factors under limiting conditions of low flow and low hydrodynamic resistance.

(c) Under the other extreme conditions, with large viscosity gradients and fast flow, they will eventually stabilize and limit the imbalance induced by the viscosity effects.

(d) They serve as useful guidelines in designing experiments. For example, if steep gradients with very dense viscous-bottom solutions are to be used, it would appear desirable to keep the ℓ_i/M considerably less than 1. It may also be desirable to choose apparatus for which all the M_i approach M. This will ensure a significant hydrostatic restoring force, according to factor (c).* (For usual experiments with small density gradients, the collection containers are kept approximately at the level of the migration chamber, and $\ell_i/M \approx 1 \pm 1$.)

(e) They suggest a way for controlling the third-dimension flow velocity profile (see Sec. IV. A, Fig. 10).

The stable steady state, and its particular significance (and, to a lesser extent, the normal pattern position,) have been stressed in various parts of the previous discussion. It should be helpful at this time to summarize the principal points relating to these two factors, for general hydrostatic-hydrodynamic situations. Well-behaved laminar flow, and density gradient stability, discussed in subsequent sections, is assumed. When not previously given or otherwise indicated, these statements follow directly from material balance considerations.

(1) A steady-state pattern requires that

$$Q^{out}_{soln\ i} = Q^{in}_{soln\ i} \text{ for all solutions i.} \qquad (18)$$

It also requires that

$$Q^{out}_{i} = \text{constant in time for each outflowing stream,} \qquad (19)$$

though all Q^{out}_i may differ from each other. Condition (18) is necessary and sufficient: condition (19) is necessary, but from a material-balance standpoint, not sufficient. Condition (18), the more general one, also implies condition (19).

(2) If $Q^{out}_{soln\ i} \neq Q^{in}_{soln\ i}$ for at least one solution i, there will be flow pattern drift. Since total liquid inflow rate = total outflow rate, during drift there must be relative accumulation and depletion of solutions in the flow-cell. In this respect the fixed-volume flow-cell acts temporarily as a source and sink for individual solutions.

---

*Possibly anomalous behavior from use of opposing density and viscosity gradients should be noted, in this connection.

This situation will arise under hydrostatic principles if a change in condition is effected, such as initiation of platform movement, or obstruction of one or more outlets. When setting up patterns with a significant viscosity gradient, the differing hydrodynamic outflow resistances have the same effect as a partial outlet obstruction and cause upward movement of the pattern.

(3) A normal steady-state pattern position requires $Q_i^{out}/Q_j^{out} = 1$ for each outflow i and j. With equal and constant individual inflows, this requires that all outflows be equal, and equal to each Q_i^{in}. The most general condition for a normal steady-state pattern position is $(\ell_i - \ell_j) =$ constant, for all i and j. A special case is $(\ell_i - \ell_j) = 0$, or $\ell_j/\ell_i = 1$. This cannot result precisely from hydrostatics alone,* as is seen from Eq. (12), or from its more general counterpart calculated from Eq. 14:

$$(\ell_i - \ell_1) = (M_i - \ell_1)\left(1 - \frac{\rho_1}{\rho_i}\right) .$$

(4) A displaced (non-normal) steady-state pattern requires that $Q_i^{out}/Q_j^{out} = \frac{d\ell_i}{dt} \Big/ \frac{d\ell_j}{dt} =$ constant $\neq 1$ for at least one pair of outflows i and j. Put somewhat differently, such a pattern requires at least one $Q_i^{out}/Q_i^{in} =$ constant $\neq 1$, with the value of this ratio indicating the displacement. That is, a ratio of 0.9, corresponding to a 10% deficit of outflow i compared with its inflow, implies a 10% (upward) expansion of this stream. This condition can arise under hydrostatic principles from density gradients [e.g. Eqs. (8) and (17)] and, according to hydrodynamic principles, from viscosity gradients.

Although a variety of ranges and combinations of the basic operating parameters has been investigated experimentally and a certain degree of optimization achieved, a complete study of all the relevant interrelationships has not been attempted. The central experimental fact remains, however, that for those parameters dictated by the physicochemical or biological requirements of a problem, the remaining essential variables could be simply chosen to provide stable flow and physical steady-state behavior of the system. Furthermore, with the usual density gradients employed to date, the steady-state pattern can

---

* Analogous to (10) and its discussion, with platform movement such that $\frac{dM_i}{dt} = \frac{d\ell_1}{dt}$, we could rigorously maintain $\frac{d\ell_i}{dt} = \frac{d\ell_1}{dt}$, or $\ell_i = \ell_1$ for all i. Even with $\frac{dM}{dt} = \frac{d\ell_1}{dt}$, this condition could be closely approximated.

generally be set up without much displacement of the strata from their "normal" geometrical positions, and with maintenance of each $\ell_i/\ell_1 \approx 1$. The pattern photographed in Fig. 3 is a good example of this.

Before concluding this section, the experimental fluid behavior, when we use a simple and convenient variant collection system, should be pointed out, because the stability arguments are modified somewhat. Experiments not requiring separate fraction collection can be conducted quite satisfactorily with one large collection vessel in place of all 12. With the commonly shared outlet liquid level, under most circumstances the flow pattern appears unchanged from that with 12 vessels. Should an outlet flow be restricted or reduced for a time, however, either deliberately or accidentally, no cumulative "error signal" builds up for that particular tube. In other words, the system still possesses flow-stabilizing feedback but lacks the cumulative individual "memory" present with the individual-vessel system.

C. Laminar Flow

1. General

It has been shown possible by the present STAFLO method to effect 100% clean separations even while violent turbulence is occurring throughout most of the main migration chamber.* Occasionally, such "limited turbulence" may even be preferred; e. g., to take advantage of this transport mechanism to speed the migration. If turbulence is present throughout the entire migration chamber, including the outlet region, however, separations and analytical transport studies are ruled out. In general, laminar flow with complete lack of turbulence is desirable. Consequently, the limiting conditions for occurrence of the laminar to turbulent flow transition are of basic importance, and some of them are discussed in this section. The role of density gradients in this regard is considered in Sec. III. D.

An excellent theoretical discussion of flow (and also of simultaneous transport of energy and mass) is given in the recent book by Bird, Stewart, and

---

*For example, the dye separation in reference 6 can be accomplished under these conditions simply by increasing the field strength until onset of turbulence in the low-conductivity middle third of the migration chamber. By the outlets, however, the separate components can be resolved at conductivity barriers--or according to other migration principles discussed in Sec. IV.

Lightfoot.[28] Although equations of motion and continuity do have wide application to ordinary incompressible fluids in turbulent motion, at present the equations cannot be generally solved. However, from a large body of studies in fluid dynamics have emerged useful semi-empirical criteria for estimating parameters associated with the laminar-turbulent transition.[28,29]

In particular, such discussions center around critical values for the dimensionless Reynolds number (Re), which is the ratio of magnitudes of inertial forces to viscous sheer forces, defined for closed conduits as

$$\mathrm{Re} = \frac{4\rho v R}{\eta} \tag{20}$$

where ρ is density in g/cm^3, v is linear velocity in cm/sec, η s absolute viscosity in poise $\left(\frac{g}{sec \cdot cm}\right)$, and R is "mean hydraulic radius," which is equal to (cross sectional area)/(wetted perimeter). For straight lengths of circular cross section pipes far removed from entrances or exits, if Re ~ 2100, flow is always laminar; if Re > 2100, it may be turbulent and at sufficiently high Re values always becomes so. Conditions for noncircular closed c nduits are less well studied but this same value of Re ≈ 2100 is commonly taken as the so-called lower critical Reynolds number. Under favorable circumstances (e.g., low-friction walls, mechanical and thermal stability, etc.), this lower critical Reynolds number can be much higher. On the other hand, nearby entrances and exits introduce often difficult-to-calculate unstabilizing influences that can disturb laminar flow.* With the present design using a rectangular migration chamber with polished lucite sides and dialysis membrane top and bottom, but with the 12 diverging inlet ducts feeding directly into the bulk solution, we shall, as an educated guess, assume Re = 2100 as an upper limit to the lower critical value and compare the customary operating Re values with that figure. (This present discussion refers to the onset of fluid-velocity-induced not electrically-induced turbulence.)

---

*It was concern over possible disruptive entrance effects on the laminar flow pattern that dictated the original flow-cell design in apparatus No. 1 with the three incoming solutions held mechanically separated for most of their passage through the cell.[6] In subsequent experiments it was shown possible to operate 12 strata with free-boundary flow the entire length of the cell, and this has been the basic design of all subsequent apparatus.[7]

Typical present extreme adverse values for the parameters in equation (20) are

$$R_{max} = 2.1 \text{ cm}^2 / 7.4 \text{ cm} = 0.284 \text{ cm},$$

$$v_{max} = 9.36 \text{ cm/min} = 0.156 \text{ cm/sec}, \text{ and}$$

$$\left(\frac{\rho}{\eta}\right)_{max} (20^\circ\text{C}) = \frac{1.00 \text{ g/cm}^3}{0.01 \text{ g/cm} \cdot \text{sec}} = 100 \text{ sec/cm}^2 .$$

(For aqueous sucrose solutions, this maximum occurs for the 0% sucrose composition.) Therefore, we have $Re_{max} = 4(0.284)\ (0.156)\ (100) = 17.7$. If we compare 17.7 with the estimated limiting $Re \approx 2100$ and bear in mind that for most operations to date $Re << Re_{max}$, there appears to be ample margin of safety for laminar flow and, in fact, judicious scale-up to considerably higher operating Re values appears reasonable. The limited experimental observations to date are in accord with this general statement. Should entrance effects eventually prove to significantly limit such scale-up for special applications, then a return to the original type of separated inlets[6] or insertion of wire mesh or other packing at the inlets could be useful.

2. Velocity Profiles and Volume Flow

In conventional steady laminar flow of an incompressible liquid through a circular pipe of radius R, the linear point velocity v_r varies axially in the familiar parabolic manner with:[29,30]

$$v_r \propto \frac{1}{R^2} \left[1 - \left(\frac{r}{R}\right)^2\right] \qquad (21)$$

where r is the radial distance measured outward from the center (see Figs. 6a and 6b). Superimposed on the isovelocity contours in Fig. 6b are inner and outer shaded areas each representing 1/12 of the total cross-sectional area. (The circular analog of the 12-channel rectangular-cross-section main-migration chamber (Fig. 2) would be indicated by including all 12 equal-area slices in Fig. 6b. Only the two sections with the extreme flow velocities are shown and need be considered for the discussion which follows.) The volume flow velocity Q in cm^3/sec for any such section is

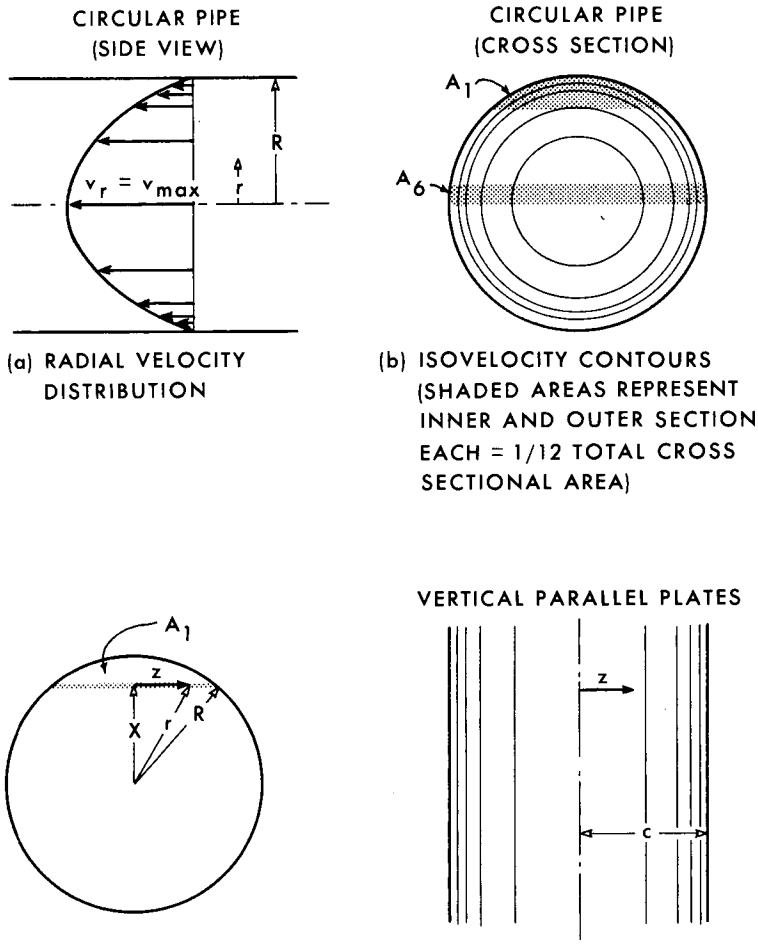

Fig. 6. Velocity distributions for ordinary horizontal laminar flow.

$$Q = \int_{x=x_1}^{x_2} \int_{z_1}^{z_2} v_r \, dz \, dx , \tag{22}$$

with the coordinates x, z, r, and R being measured for a very thin section as indicated in Fig. 6c. The limits of z for the first integration are seen to be $\pm (R^2 - x^2)^{1/2}$ but the limits of x for the second integration remain to be determined. By introducing the z limits, substituting v_r from Eq. (21), replacing r by $(x^2 + z^2)^{1/2}$, and performing the first integration, Eq. (22) becomes

$$Q = C \int_{x_1}^{x_2} (R^2 - x^2)^{3/2} \, dx, \tag{23}$$

where C contains only constant terms common to all such sections. To evaluate x_1 and x_2, we refer to the formula for the area of a segment of a circle (e.g., area A_1 in Fig. 6b and 6c):

$$\text{area} = R^2 \cos^{-1} \left(\frac{x}{R}\right) - x \sqrt{2x(R-x)} \tag{24}$$

Setting Eq. (24) equal to any desired fraction of the total area πR^2, we can solve by successive approximations or by series expansion to obtain x in terms of R. With the limits thus obtained, Eq. (23) can be integrated and evaluated for the flows Q_1 and Q_6. The end result of this calculation is that the outer section flow Q_1 is only about 40% of the inner flow Q_6. (By way of comparison, a calculation for flow through the outer annulus having 1/12 the total area shows it to be less than 5% of the flow through the central core of the same area. The larger discrepancy between these two results from the greater average proximity of the outer annulus to the wall, where the velocity drops to zero.)

Cornish[31] has derived an expression for the point velocity in laminar flow for a long rectangular conduit of height 2a and horizontal depth 2c:

$$v \left(\frac{cm}{sec}\right) = \frac{32}{\pi^3} \frac{c^2}{2\eta} \frac{dP}{dy} \sum_{n=0}^{\infty} \frac{(-1)^n}{(2n+1)^3} \frac{\cosh (2n+1)\pi x/2c}{\cosh (2n+1)\pi a/2c} \tag{25}$$

$$\times \cos (2n+1) \frac{\pi z}{2c} - \frac{c^2}{2n} \frac{dP}{dy} \left(1 - \frac{z^2}{c^2}\right)$$

(Here, x and z are the vertical and horizontal coordinates respectively, measured outward from the center of the conduit, $\frac{dP}{dy}$ is the pressure gradient in the direction of horizontal flow, and η is the viscosity.) There appears to be a discrepancy,

however, between the assumption of zero pressure gradient in the x and z directions used to derive this expression, and Nikuradse's experimental results, interpreted in terms of certain inner circulation patterns.[32, 33, 34*]

Aside from this point, for other reasons it is not deemed worthwile to undertake the same kind of calculation just made for the circular cross section using Eq. (21), but now using instead the more complicated expression (25).** For one thing, a qualitatively similar result will hold, as is known from Nikuradse's measurements of velocity profiles for a number of noncircular cross sections. His work showed that the isovelocity contours are no longer symmetrical, (analogous to Fig. 6b) but vary in shape from the center to the outside, bending outwards at the corners.[34] This presumably gives rise to a kind of local outward circulation resulting in a somewhat increased flow near the walls, compared with the circular case. Nevertheless, the conclusion still holds that volume flow through the top or bottom 1/12 is considerably lower than that for a middle 1/12 of the cross section. A second reason not to make this calculation using (25) is that it would not take account of the realistic conditions during STAFLO experiments, where viscosity and density gradients (and entrance effects) are present.

We can summarize this flow profile discussion as follows. Although neither the theoretical nor the experimental analyses of flow outlined above are directly applicable to solutions usually present inside the main migration chamber, they do serve as a useful basis for qualitatively contrasting ordinary laminar flow with STAFLO flow. They indicate that with ordinary laminar flow, in the absence of the stability principles described previously, average steady-state volume-flow rates through the extreme tubes No. 1 and No. 12 should be considerably less than for the central tubes No. 6 and No. 7. Since this is not the case, we can say that these stability principles have been "strong" enough to override the usual velocity relations of ordinary viscous flow and strong enough to override effects of

---

*With such circulation, $\frac{\partial P}{\partial x} = 0$ and $\frac{\partial P}{\partial z} = 0$ should not hold.

**To eliminate the pressure gradient in expression (25), we integrate it over the cross section. This gives an expression for the pressure gradient in terms of total volume flow which can be substituted back into expression (25).

nonuniform density and viscosity in changing these usual relations, and they give rise instead to a stabilized kind of plug laminar flow in the vertical sense.* Study of steady-state patterns, such as in Fig. 3, has revealed no systematic vertical distortion of this condition near the top or bottom, at least down to the level of a single layer thickness (though, of course, precisely at the stationary top and bottom membranes, the flow rate must be zero). Hence, the flow pattern might be expected to approach the parabolic form applicable to a single liquid between two infinite parallel plates, with isovelocity contours parallel to the vertical walls as in Fig. 6d. The possible implications of the horizontal (z direction) velocity profile on STAFLO migration are discussed in Sec. IV.

3. Set-Up Problem

The above discussion has been concentrated on the maintenance of the steady-state laminar-flow condition. Let us consider briefly the experimental problem of setting up a steady-state pattern. Initially, the entire system is filled with water which is to be displaced by the 12 inlet solutions having generally higher density. Under equilibrium conditions in the limit of very slow flow, these denser solutions, upon entering the cell, should sink to the bottom and flow out the lower outlets then slowly rise toward their proper vertical positions in the cell, setting up the desired vertical density-gradient condition. However, the same viscous forces previously described considerably speed up this process. With initial total flows of the order of 15 to 30 cc/min (or 10 to 15 cm/min) and with sucrose gradients even as small as 0 to 2%, hydrodynamic resistance is sufficient to cause the denser solutions to rise upward rather quickly. This forces the water out into the collection bottles, with the individual streams under laminar flow retaining their layered positions relative to each other. To speed up this process even more and to conserve solutions, the lower outlets can be shut off for a short time, rapidly forcing up the entire flow pattern in a regular manner toward its normal steady-state position. In this fashion, the steady-state pattern can be

---

*This velocity independence in the vertical sense stands in contrast to the work reported by Philpot as he clearly states that his horizontal flow velocity "S" is a function of the vertical height in the cell, "Z."[16] Other attempts have been made to equalize outflows by adjusting outlet pressures (e.g., heights of free tips of outlet tubing). These attempts have been unsuccessful because of the inherent instability of such a configuration.

established by the time that hardly more than the first throughput volume has flowed. Figure 7 (Plate I) is a photograph of the dye system of Fig. 3 taken during the setup time. The striped pattern (which upon first entering the flow-cell fell and was all compressed into a thin layer at the bottom) is seen to have moved about half of the way up to its "normal" position.

Other methods for establishing the time-independent flow configuration may also be utilized. With the separated channel inlets of the original apparatus No. 1,[6] much faster initial flow can be employed, literally pushing out the lower density water ahead of it. Though this leads to considerable turbulence near the inlet of each individual channel, flow rates can be selected such that laminar flow is established before the free-boundary portion of the migration chamber is reached. In the present 12-channel apparatus, initial high-speed turbulent flow can also be employed to purge the system of water. In spite of the resultant mixing between adjacent streams, an approximately correct density gradient can be simply established in this manner. Then, by slowing down to usual operating flow rates, the freshly entering pattern immediately becomes almost ideal. The principal disadvantage of this latter setup method is that it is more wasteful of solutions and since the method of Fig. 7 can be accomplished in about the same time, it is generally the method of choice.

After the steady-state flow pattern has been established, it is possible to make substitutions for one or more inlet solutions with little or no disturbance, if the substitute stream's density is intermediate between those of the streams immediately above and below. This technique is particularly useful when only a small amount of a valuable sample is available, for it minimizes waste during the setup.

The steady state described here refers to the hydrodynamic steady state, but where "force fields" other than normal gravity or chemical concentration gradients are of importance, a steady state must also be established with respect to all the other variables. It is sometimes more convenient to set up an electrophoretic steady state after the hydrodynamic one, though both can be done simultaneously if desired.

The laminar-flow properties described in this section permit some other interesting and sometimes useful variant modes of operation. Individual outlet valves can be partially or totally shut off, leading to relative displacement of adjacent streams without disturbance of their laminar-flow characteristics. In this manner, spacing between adjacent streams can be arbitrarily increased or decreased; this is useful, for example, to force certain components out certain

Fig. 7. See Plate I (page 10).

specific exits, to increase spacing between two very close components, or to force two or more components out the same exit. Subject to such manipulations, the various streams appear to behave like flexible elastic bands. The pattern as a whole can be relatively compressed or expanded by operating with 11 adjacent open outlets and 12 inlets, or vice versa. This, of course, leads to velocity gradients inside the flow cell, (which may be useful for special applications), but within wide limits this can be tolerated without destruction of the laminar-flow pattern. The flow-stability principles previously described are still operative, though they are now also subject to the imposed outside constraints, meaning that stable flow (for a given flow rate) no longer implies the same relation between collection-bottle levels as before.

D. Density-Gradient Stability

1. General Initial Stability

An aspect of stable flow (in the broad sense) is the hydrostatic stability of solution density gradients in a gravitational field, subject to diffusion and other external forces. Convection arising from instability of this kind will interfere with or destroy the uniform pattern established or to be established under the flow-stabilizing principles previously described; such convection will have a deleterious effect on desired preparative or analytical studies. To simplify the present discussion without overly restricting its general validity, we will neglect direct interaction of such convection with the flow itself.

To state the obvious physical fact, a macroscopic fluid volume element of higher density than that of the solution beneath it tends by convection to reverse this density instability. Other forces may oppose this tendency, e. g., magnetic (as shown by Kolin[35]) or surface (adsorption), but they will not be discussed here.*

More precisely, for stability, slopes of curves of increasing density (ρ) versus increasing height (x) must everywhere have

$$\frac{dx}{d\rho} < 0 \quad \text{or} \quad \frac{d\rho}{dx} < 0 . \tag{26}$$

*A possible indirect involvement of the electrical force (during electrophoresis) is, however, mentioned in Sec. III. D. 3.

Basically, we wish to know the relationships between the physicochemical properties of solutions, both background buffer (solvent) and superimposed solute, and density-gradient stability, all during the migration process. For example, we would like to be able to calculate the detailed properties of the density gradient necessary to support a given amount of specified protein or cell sample under given migration conditions. In addition, maximum and minimum sample capacities are important to know.

A major difficulty in theoretical analysis of gravitational stability of solution density gradients is that exact calculations of simultaneous diffusion, convection, electrophoresis, heat conduction, and sedimentation are not presently possible. In complex systems of this sort, one usually must settle for approximate calculations on simplified models using idealized force laws. Such calculations may still be useful in estimating practical limiting conditions. Already Philpot[16] recognized their importance and made some estimates of limits, and Svensson and co-workers[36] have considerably extended this line of work. Svensson, in an excellent review, also describes other previous contributions to this field.[15]

It is convenient to subdivide the problem as follows: (a) initial gravitational stability of density gradients subject to diffusion only; (b) time changes of stability; and (c) effects of other force fields (especially electrical and thermal).

Initial stability. We must simply choose our starting solutions to satisy the criterion of Eq. (26). Svensson has stressed the usefulness of "density diagrams" for such stability discussions.[15] Referring to the hypothetical height-density curve in Fig. 8, we see that regions cd and ef are unstable. In order to set up desired initial density gradients in usual batch processes such as density-gradient electrophoresis, a variety of gradient mixing devices has been described.[15] With the STAFLO method, however, one can closely approximate virtually any desired gradient not only that of density but also simultaneously and independently those of conductivity, composition, etc., about as easily as one can fill the apparatus with water. The 12 appropriate solutions are simply fed into their respective inlets, and at suitable flow rates and by use of thin layers, the discontinuities at the free boundaries are smoothed by diffusion sufficiently quickly for most purposes.*

*It is also possible to employ controlled laminar flow "crossing over" of inlet streams by deliberately introducing them in the sense contrary to condition (26); this has sometimes proved useful.

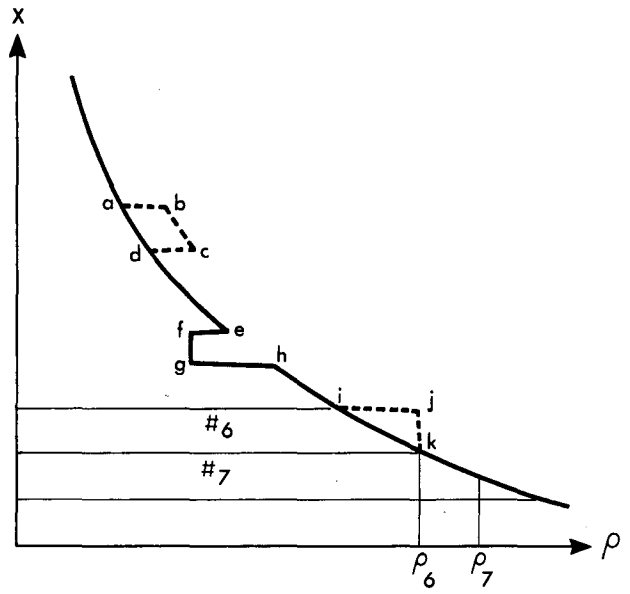

SOLID CURVE : CONTRIBUTION OF BACKGROUND SOLVENT
DASHED CURVE : OUTLINE OF CONTRIBUTION OF SAMPLE

MU-29021

Fig. 8. Hypothetical curve of total density vs height in a uniform vertical vessel.

2. Time Changes

The addition of a sample to one or more inlet solutions, albeit in a manner initially consistent with condition (26), immediately introduces stability complications for future times. For example, a protein sample solution of initial density ρ_6 from inlet No. 6, such as region ijk in Fig. 8, must contain less density building solute (sucrose) than No. 7 with average initial density ρ_7 and containing no protein, in order to have $\rho_6 < \rho_7$. With such two-way concentration gradients and with the diffusion coefficient for sucrose considerably larger than that for a typical protein, the faster diffusional influx of sucrose in No. 6 compared with its outflux of protein may for certain times give rise to the unstable condition $\rho_6(t) > \rho_7(t)$, where the densities are now considered functions of time. The experimental manifestation of this instability is the formation (at the boundary) of the "sedimenting droplets" described by Brakke[37] and others.[15] It has been counteracted mechanically[37] or by judicious choice of solutes with proper diffusion coefficients.[15]

Such droplet sedimentation has also been noted in certain STAFLO experiments, in qualitative agreement with Brakke's competitive diffusion model. It was furthermore observed in previous nonflow experiments of the author, using Kolin's U-tube microtechnique,[38] indicating that even a very large "density shelf," as suggested by Svensson,[15] is not necessarily sufficient to prevent such diffusion-induced convection. Droplet sedimentation has not been a problem or limitation in studies with the STAFLO method and, in fact, it has led to some interesting experiments which will be reported later. A somewhat related kind of instability that may be called "bombing" has proved to be a factor in STAFLO cell-migration studies and is discussed below and in Sec. IV. A.

In analyzing the density change resulting from an initially stable sample band in a solution density gradient of different composition, Svensson, Hagdahl, and Lerner[36] concluded that density changes at the center of even a thin sample band could be ignored compared with those occurring at the interfaces. Using some simplifying assumptions, including ideal diffusion, a small background density gradient established by a single solute, and a very thin initial sample, they calculate for the band interfaces that

$$\frac{d\rho}{dx} = \mp \frac{1}{2\sqrt{\pi t}} \sum_{i>1} \Delta c_i (1 - \bar{v}_i \rho_0) \left[\frac{1}{\sqrt{D_i}} - \frac{1}{\sqrt{D_1}} \right] , \qquad (28)$$

where the minus sign applies to the upper interface, the plus sign to the lower; the distance x is measured positively upwards from the interface;*

*Svensson used the opposite sign convention.

the summation is made over all solutes i except for $i = 1$, the principal gradient-producing solute; ρ and ρ_0 are densities of solution and solvent, respectively; t = time of diffusion; Δc_i = concentration increment for the ith component across the interface (positive if c_i is higher in the sample band); $\bar{v}_i$ = partial specific volume for the ith component; and D_i = diffusion coefficient for the ith component. For a macromolecular solute band in an initially stable sucrose gradient, all terms in Eq. (28) are positive so that for $t > 0$ the lower interface is gravitationally unstable, hence we have droplet formation. This same argument holds for cellular or subcellular samples too small or too light to sediment appreciably under 1 g. However, by addition of auxiliary solute or solutes having appropriate Δc_i, $\bar{v}_i$, and D_i, either to the sample band or background solution, this sum can be set equal to zero, thus, in principle, eliminating the instability.

Equations of this form are a useful basis for a discussion of the elements contributing to diffusion-convection stability at a boundary. However, because of the limitations of the approximations involved in deriving equation (28), and because of lack of suitable data, this equation cannot be expected to be quantitatively valid for choosing stabilizing concentrations of auxiliary solutes.[15] Though refinements could be made to the equation, and to others of this type,[16,15] our primary concern is the stability during migration processes such as electrophoresis and sedimentation, which we have not yet taken into account. These transport processes, in fact, enormously complicate the theoretical analysis, for in addition to diffusion, we now have possible simultaneous mass transfer by electrophoresis, sedimentation, and heat-induced convection (from the passage of current).

Living cells as large as a few microns in size can sediment across a supporting sucrose solution interface sufficiently rapidly to prevent diffusion-induced instability. On the other hand, in STAFLO experiments of both yeast and blood cells, this very sedimentation is sometimes associated with another kind of instability called "bombing" which, for given solution conditions, appears to depend strongly on two factors: (a) the number of cells/cc, and (b) the state of dispersal or aggregation of the cells in the sample suspension, and also, to a lesser extent, on a third factor, the nature of the density gradient. When this "bombing" occurs, visible clumps of cells break away from the sample stream entering the main migration chamber and rapidly sediment downward. These groups are usually loose enough to leave a trail of cells behind, clearly marking their trajectories. The trails generally start at or near the inlet end and continue for a certain time (downstream distance) after which the solutions commonly become stabilized against this behavior. In the yeast sedimentation experiments to be described subsequently,[39]

this "bombing" could be expected with sample concentrations above $\approx 4.3 \times 10^7$ cells/cc, representing volume fractions of $\lesssim 5\%$. In similar more recent experiments with larger mammalian bone marrow cells, the limiting cell concentration for this phenomenon appears a little lower, the limiting volume per cent somewhat higher. (These trails can be very useful as "tracers" for visualization of the velocity profiles in the migration chamber and also to mark density discontinuities by their relative accumulation at these positions.)

In effect, at these cell concentrations, the cells in the "bombs" have ceased to sediment as independent entities but now move in groups.* In other words, in the absence of bulk instability, or diffusion induced convection,** for small "macroscopic regions," $d\rho/dx > 0$ does obtain. From the observed filament-like trail of sedimenting yeast "bombs," the sedimentation appears to be neither of intact droplets nor of clumps held together by strong forces (as with clumpy strains) but rather something in which weak forces are involved. This behavior could arise in several ways. Even in a "well dispersed" culture, there is a statistical randomness in distribution of cells/unit volume with the variation the greater the smaller the volume considered. Thus, with a cell suspension just barely meeting the bulk stability criterion, slight local fluctuations in density could lead to this behavior. One might also expect much worse "bombing" with less well dispersed suspensions or with cells tending to stick or clump together, and this is precisely what happens. In bone-marrow cell experiments the state of nonrandom distribution, as measured in a hemocytometer, was directly related to the mechanical measures taken to disperse the marrow jel and also to the variations in specific ionic composition of isotonic suspending solutions. This nonrandomness corresponded very well to the observed "bombing." (To quantitate this relationship one could measure the deviation of the single-cell grouping, seen in the hemocytometer from a Poisson distribution, for fractions containing the "bombs." The different size sedimenting clumps generally arrange themselves vertically by clump size, and can be separately collected in sedimentation-velocity

---

*In so doing, they must of course carry with them a small amount of entrapped liquid.

**Under some circumstances, net upward diffusion of small molecules like sucrose into the sample region could be a contributing factor; from experiments with different sucrose gradients and substitution of dextran, it appears not to be the major one, however.

experiments.) "Stickiness" of these mammalian cells is much greater than for the yeast strains used so that with marrow bombs the cell "trails" are generally lacking or greatly reduced. Other possible origins of the phenomenon include (a) the local increase in cell concentrations just below the sample region, or at a "density shelf" which has not been sufficiently smoothed out by diffusion, and (b) cell pile-up on small ledges acting as inlet flow dividers, if the apparatus was not designed to eliminate this cause.

In this behavior of a fairly sharp cutoff concentration (cells/cc) for the change of condition of suspension, the system bears a certain resemblance to that undergoing a phase change. With its apparent strong dependence on the state of aggregation (e.g., forces between components), such a system suggests itself as a sensitive tool for studying such aggregation of forces.* In STAFLO experiments focusing on the properties of the individual cells rather than on clumps, to reduce or eliminate this bombing yet operate with the highest possible cells/cc, the instability concentration is generally determined experimentally, then a slightly lower concentration employed.

3. Effects of Other Force Fields

In the presence of an applied external force, such as an electric field, the situation becomes quite different. A gravitationally unstable macroscopic region of solution of high cell concentration, can be stabilized by an upward electrical force on some or all of the cells, so that different and more complicated stability conditions are applicable. On the other hand, Joule heat dissipation associated with the flow of current can give rise to convectional instability. To estimate limits on the temperature rise associated with current flow, we first calculate the power in watts, w, dissipated in volume $A \cdot x\,(cm^3)$:

$$w = \int_0^x \frac{i^2}{kA}\, dx, \tag{29}$$

where i is the current in amps, $k = \frac{1}{r}$ is the specific conductivity in $ohm^{-1}\,cm^{-1}$, A is the cross sectional area in cm^2, and x is the height in cm of the rectangular volume.** Though for many applications of the STAFLO method, k is a function

* For example, in this manner, one could easily follow sedimentation of whole blood, and the influence of specific protein or ionic species, in the sample stream or in streams beneath, in the path of sedimentation.

** This follows directly from the fundamental relations, $dR = \frac{r\,dx}{A}$ and $dW = i^2\,dR$ with dR the resistance in ohms, and r the specific resistivity in ohm-cm, of the volume element.

of x, for this approximation we integrate simply for k (and A) constant, and we also ignore the temperature dependence of k. Expressing the result, using appropriate intensive quantities, we have

$$\tilde{w} = 0.239 \frac{\tilde{i}^2}{k} = 0.239 \tilde{E}^2 k, \tag{30}$$

where $\tilde{w}$ is in calories/cm^3, $\tilde{i}$ is the current density in amp/cm^2, and $\tilde{E}$ is the field strength in volts/cm. If the flow-cell itself were completely adiabatic, the inside temperature for each volume element would rise at the rate $\frac{\tilde{w}}{\rho \tilde{c}_p}$ to a maximum steady-state value at the outlet of

$$\Delta T(^\circ C) \approx \frac{0.239\, \tilde{i}^2 V}{k \rho \tilde{c}_p Q} \text{ or } \frac{0.239\, \tilde{E}^2 k V}{\rho \tilde{c}_p Q}, \tag{31}$$

where $\tilde{c}_p$ = solution specific-heat capacity in cal/g·°C,

ρ = solution density in g/cm^3,

V = total migration-chamber volume in cm^3, and

Q = the constant total flow rate in $\frac{\text{cm}^3}{\text{sec}}$

To evaluate this expression for some typical operating conditions, we can choose

$$\tilde{i} = 10^{-3} \frac{\text{amps}}{\text{cm}^2},\ k = 10^{-4} \text{ ohm}^{-1} \text{ cm}^{-1},\ \tilde{E} = 10 \text{ volts/cm},$$

$$V = 63 \text{ cc},\ \frac{V}{Q} = 2000 \text{ sec},\ \rho \approx 1 \frac{\text{g}}{\text{cm}^3} \text{ and } \tilde{c}_p \approx 1 \frac{\text{cal}}{\text{g}\cdot^\circ\text{C}}$$

Therefore, from Eq. (31), we have $\Delta T \approx 4.8^\circ$C.
This result should be approached at sufficiently high, vertically uniform flow rates.* At sufficiently low-flow rates, other conventional mechanisms of heat transfer will predominate, while at intermediate flow rates all causes may contribute significantly to the heat loss. Conduction and radiation losses through the walls depend strongly on the material and geometry of the flow-cell.

If heat produced according to Eqs. (29) or (30) and the temperature rises [Eq. (31)] occur uniformly throughout the main migration chamber, density stability should not be disturbed. In general cases, however, only V must always remain constant (for a given apparatus) so that variations in the other

*Dobry and Finn discuss the applicability of a similar equation to their vertical nonuniform forced-flow situation.[14]

factors (particularly k) could give rise to temperature gradients inside the apparatus. If the resulting local density changes lead to a reversal of the basic stability condition (26), or to the analogous one in the horizontal direction, some convection will then occur. A properly constituted density gradient can counteract or limit this convection to a small region of solution.

The data in Table II indicate the magnitude of the temperature-induced density change for water in terms of the equivalent sucrose density gradient. Thus, to the first approximation, a 0 to 2% linear sucrose gradient would just imitate a 45°C to 20°C linear-temperature distribution over the same distance. We can also consider the situation from the inverse standpoint. That is, experiments employing a 0 to 2% sucrose concentration gradient for density stability have alternatively been successfully conducted without sucrose but with a 25°C externally imposed temperature difference across the solutions as was reported in the original STAFLO communication.[6]

In addition to the temperature effect on density profiles, heat denaturation of sensitive biological samples remains a distinct possibility with any kind of electrophoresis, as pointed out by Philpot[16] and numerous other investigators in this field, and must be taken into account in the design of the original experiment. As a kinetic process, such denaturation of course depends on time as well as temperature. Relatively higher temperatures may be quite acceptable biologically for short times in the STAFLO apparatus (e.g., protein separations have been accomplished with less than five minutes in the electric field) that would be completely ruled out in other types of electrophoretic apparatus with experiments lasting many hours. Note that the average temperature rise of a sample passing through the STAFLO apparatus would only be half that given by an equation like Eq. (31).

More complete analysis of heat-transfer mechanisms will not be given at this time. Suffice it to say that for experimental work to date no thermostating or cooling has been necessary either to prevent convection or to preserve biological activity. For future scale-up to maximum current densities and maximum preparative sample capacity this may be desirable or required.*

Quite apart from heating effects during electrophoresis, one must also consider the direct effect of the sample migration on the density profile and its stability. For example, if an initially stable sample occupying the "hole" efgh in the density gradient of Fig. 8 moved up to position abcd as shown, its lower

---

*A very simple initial step for cooling would be to employ countercurrent flow through the top and bottom electrode compartments.

Table II. Equivalent temperature and sucrose contributions to aqueous solution density.

Weight % Sucrose	0	1	2	3	4	5	6
T (°C)[a]	20	34	45	53	61	69	76

[a] T = temperature of water having percentage density decrement (relative to water at 20° C) equal to the percentage density increment from the corresponding sucrose concentration.

boundary cd would be unstable. For thin electrophoresing sample regions in density-gradient columns under certain restricted conditions (e.g., neglecting diffusion, electric-boundary spreading, horizontal temperature gradients, etc.), Svensson et al.[36] calculate the form of the sample density distribution and concentration distribution, c(x) which would be everywhere compatible with the basic stability condition (26). This also provides a convenient basis for discussing maximum sample capacity.

From the exact expression

$$\underline{m} = \int_0^h c(x)dx,$$

with c(x) in g/cm, he obtains as a first approximation to the integral,

$$\underline{m}_2 \leq \frac{V(\Delta\rho_0 - \Delta_w\rho)}{2(1 - \rho_0\bar{v}_2)} \tag{32}$$

where $\underline{m}_2$ = mass in grams of solute in a sample region of V cm^3 and h cm high, $\Delta\rho_0$ = the (small density difference across h, $\Delta_w\rho$ the supposedly known smallest density difference compatible with the given $\tilde{w}$ [see Eq. (30)], and ρ_0 and $\bar{v}_2$ as defined for Eq. (28). Since $\underline{m}_2$ is a maximum sample mass per volume V, equation (32) in a sense also gives a measure of possible sample capacity in a static density-gradient column under the defined conditions. However, mass per unit time is perhaps a more fundamental capacity measure, The presence of flow rate as an additional variable has important implications for capacity defined in the latter sense. Rather than maximize $\underline{m}_2$ or $\underline{m}_2/V$ as suggested by Eq. (32) it may often be preferable to operate with lower $\underline{m}_2/V$ (g/cm^3) but higher Q (cm^3/sec) to achieve a higher product of the two factors.* Possible advantages include:

(a) Shorter sample-handling time, reducing normal stress of handling, or alternatively allowing greater deviation from ideal biological conditions for the shorter time.

(b) Simplification of the heat-removal mechanism by favoring flowing-fluid removal. (In experiments where cooling is important and takes place essentially

*Should resulting separated fractions be too dilute for certain purposes they can be quickly concentrated by subsequent STAFLO electrophoresis or sedimentation or by ordinary centrifugation.

by fluid flow, then a large increase in capacity by increasing the channel width is possible, whereas the corresponding increase in diameter of a static column is precluded.)

(c) Higher electrophoretic mobilities generally obtain at lower ionic strengths (see Sec. IV. B. 2). For lower protein concentrations, lower ionic-strength buffers can often be employed without exceeding solubilities, further simplifying heat-production problems.

(d) Simplification of molecular-transport mechanisms (e. g., de-emphasis of diffusion or sedimentation relative to electrophoresis).

Also in a steady state flow system, the total mass of sample can be increased arbitrarily by increasing the time. For batch-type density-gradient columns, equations like (28) and (32), which are admittedly an oversimplification of the physical situation near the beginning, should become increasingly bad approximations as time goes on. Furthermore, if only thin narrow sample zones are of practical importance in nonflow zonal electrophoresis[36] [inherent in the derivation of Eq. (32)], in the STAFLO method wide sample zones can sometimes be used to increase capacity and to effect simultaneous concentration of fractions with their separation. For additional discussion of this point see Sec. IV. A.

Because of the difficulties pointed out in this section in realistic theoretical analysis of density-gradient stability, the value of the experimental approach should be stressed here. Experience with the STAFLO method has shown that instabilities that should exist or develop according to the arguments presented here frequently do not develop or are quickly corrected, and that "Le Chatelier" type principles of opposing forces, or internal compensation, appear to be operative. As a result, favorable stability relations for a given migration problem have usually been obtainable empirically with relatively little difficulty. Svensson[15] reported the same fortunate experience for his column electrophoresis experiments, noting for example, "... the original concentration distribution, if not compatible with convection-free migration, is capable of adjusting itself...". The value of the simplified theory in correlating and interpreting the results and in designing experiments remains, however, and will increase as more basic data become available and more sophisticated analysis is forthcoming.

IV. MIGRATION PRINCIPLES (AND MIGRATION)

A. General*

We will first restrict consideration to a uniform flow field throughout the three-dimensional volume, the velocity to be represented everywhere by a single horizontal vector. In response to an applied vertically acting force field (Fig. 9a), migration of components follows some resultant vector path, such as 1 if vertical migration is uniform, or 2 if nonuniform. Mixtures of components can then be resolved by the outlet system, 0, according to a variety of principles, some of which are indicated for two components in Figs. 9b through 9e.† Broadly speaking, these principles can be considered thermodynamic or equilibrium if, by the time they have reached position 0, the slope of the resultant sample migration vector is zero; they can be considered kinetic or rate if it is not zero. Even in the former case, many nonequilibrium (yet steady-state) processes may be occurring, however.

In Fig. 9b, two components with differing constant generalized "mobilities" (in a uniform force field) follow distinct straight-line paths to separate outlet positions. This could represent Tiselius-type free-boundary electrophoresis, or uniform sedimentation, both leading to rate migrations and separations. Figure 9c depicts different mobilities of components until they have reached "migration barriers" in solution whereupon the mobilities appear to drop to zero. This is easily accomplished in free solution electrophoresis by use of a "conductivity barrier." By having the solution electrical conductivity below p and above p' considerably greater than that between p and p', the field strength decreases markedly at these positions. Migration to positions p and p' is kinetic; beyond that migration is equilibrium, although because the transference number of components 1 and 2 can never drop completely to zero at p and p', the latter is only approximately true. The components can also become immobilized by chemical changes occurring when they reach solutions of differing composition at p and p' (equilibrium). Uniform sedimentation or flotation to a position of a strong density discontinuity ("density shelf") also can give rise to such migration paths.

---

* Generalized stable-flow free-boundary migration may be called STAFLO-phoresis. Similarly we have used more specific designations such as STAFLO-sedimentation and STAFLO-electrophoresis.

† By application of standard optical techniques, continuous analytical procedures can also be performed simultaneously.

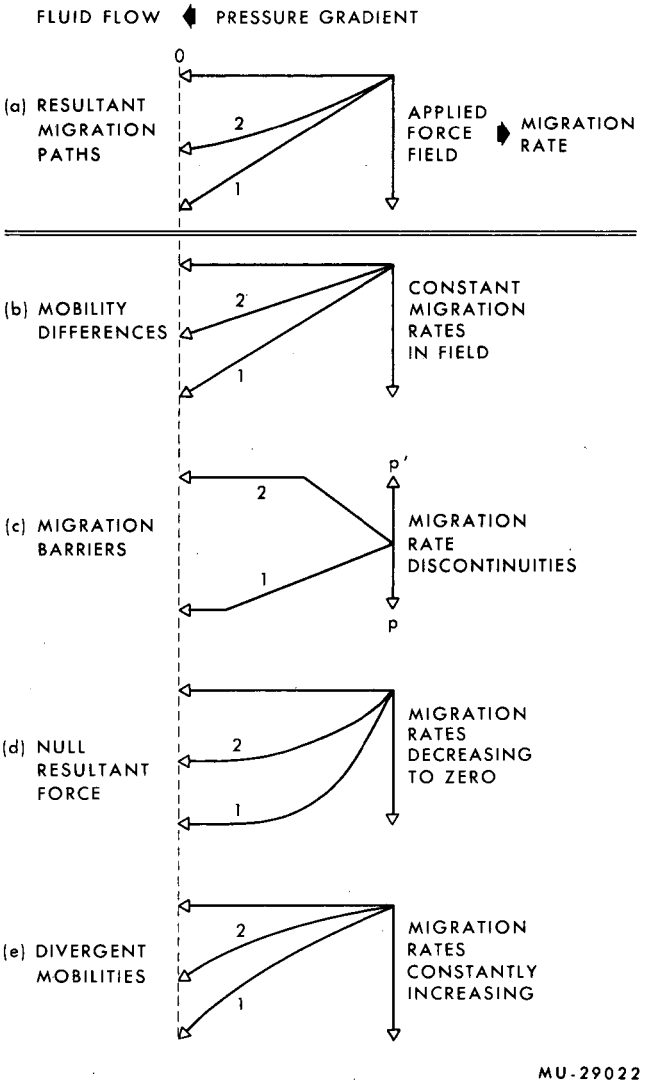

Fig. 9. Migration principles in a uniform flowing system.

In Fig. 9d, migration rates are continuously decreasing and reach zero at the components' equilibrium positions. This can arise with species of fixed properties migrating in a variable force field, e. g., sedimentation or flotation in a density gradient. It can also arise from the changing properties of species migrating in either a uniform or nonuniform field. An example of this latter is electrophoresis of amphoteric substances in a pH gradient. As originally reported by Williams and Waterman,[40] who established the pH gradient through passage of the current itself, with proper polarity the ampholyte becomes immobilized at its isoelectric point. In applying the principle to U-tube microelectrophoresis, Kolin established the gradient by use of different solutions, and by combining this with strong conductivity and density gradients, achieved much more rapid migrations as described in detail in his review article.[41]

Kauman,[42] in Prigogine's laboratory, has considered some of the theoretical aspects of this type of migration. Major unsolved problems remain, however, in understanding total behavior of buffer or other non-sample solutes during the passage of current. This is particularly serious for batch electrophoresis where the pH profile distortion will be the greater, the longer the experiment. Only for special buffer systems will this pH drift be minimized.* On the other hand, with the STAFLO method even with very large migration of pH-determining ions the pH profile in solution becomes time independent so duration of experiment is not thereby limited. Also, since accurate theoretical calculation from first principles of such profiles in complex buffer systems migrating in electric fields is impossible, the STAFLO approach is particularly useful for investigating the nature of the transport processes experimentally. In recent work at our laboratory (to be reported in detail later) it was found possible to establish highly reproducible, uniform, stable pH gradients in buffer systems flowing through the electric field, and thereby gain some insight into the details of the migration itself.

Closely related in concept to isoelectric point stabilization through pH equilibrium with ampholytes is the interesting work reported in a series of papers by Schumacher and collaborators on "focusing" electrophoresis.[44,20] Working mostly with inorganic ions on paper, they cause them to migrate rapidly from both directions to quasi-stable positions determined by various equilibria, such as complexing reactions, etc. Extension of these methods of STAFLO experiments could be very profitable.

---

* Svensson[15] has pointed out the value of buffer gradients made from a uniformly distributed salt, with a variable-concentration uncharged weak acid or base corresponding to one of the salt ions. He also reports current progress in a series of papers on natural pH gradient.[43]

The relation between the different migration principles, represented by Fig. 9b and Fig. 9d, and preparative sample capacity should be mentioned here. Sample mixtures migrating in a kinetic mode (Fig. 9b) should start from a thin sample region in order to be completely fractionated by the end of the experiment. Under mode 9d, however, components could move to the positions indicated regardless of point of origin in the flow cell; hence, the initial sample region could be very broad. All other factors being equal, therefore, cc or mg of samples flowing per unit time should be greater under the conditions shown in Fig. 9d according to the ratio of the initial sample-band thicknesses (measured in integral numbers of inlets). Furthermore, each component would be concentrated under 9d according to the similarly measured ratio, the original sample-band thickness per final component-band thickness (up to a maximum concentration factor of 12 for a single passage through the present apparatus). All other factors are not necessarily equal, however, and for a given mixture, a sufficiently faster flow rate might be possible under 9b to more than compensate for its reduced volume in the apparatus. If, for example, one component had zero mobility, it could generally not be completely separated under 9d using a wide sample band, for some would be present in any fractions concentrating inside the boundaries of the original sample band.

Problems that can arise in density gradient columns from low solubility, (as for certain ampholytes at their isoelectric points), have been pointed out.[15] In STAFLO experiments to date, by use of supporting density "shelves," by adjusting parameters to cause the "precipitation" just before the outlets, or simply from avoiding precipitation by the short throughput times for samples, such difficulties have been easily surmountable.[7]

Divergent mobilities as in Fig. 9e will arise from 9d situations if the driving-force polarity is reversed; they can be useful in obtaining the most rapid migrations. With such polarity, however, a given ampholyte could migrate in a pH gradient either to the cathode or anode depending upon the pH profile in solution relative to its isoelectric point, so care must be exercised in such experiments.

Another migration principle pertinent to cell sedimentation studies is inherent in the observed cell "bombing" previously described in III. D. 2. If the cell aggregates were on the average somewhat enriched in larger (faster sedimenting) cells (which is reasonable since these would tend to concentrate in the initial lower portion of the entering original sample region faster than would the smaller cells), the whole sedimentation pattern would be spread out, yet still qualitatively tend to

maintain the relative spatial distribution of the individually sedimenting cells. Furthermore, since the clumps are not "closed" but break up during their trajectories, individual sedimentation continues after that time thereby enhancing the downward enrichment of the faster cells. Thus, a combined kind of microconvection and individual sedimentation would be operative, which might descriptively be called "grav-chromatography" and which, under favorable circumstances, could aid the separation. There is evidence that this was a contributing factor in the yeast sedimentation that we are discussing.[39]

The migration principles described thus far often can and will be applicable more than one at a time for any given force field. Also, more than one type of force field can simultaneously be effective; e. g., vertical sedimentation and electrophoresis of cells (IV. B. 3).* Furthermore, with a two-dimensional array of outlet tubes, simultaneous action of two different driving forces (e. g., electrical, inertial, magnetic,[46] thermal) at right angles to each other and to the flow was suggested[6] though no practical use has yet been made of this principle. Finally, to take maximum advantage of the many different migration principles, for both preparative and analytical purposes, considerably more experimental and theoretical work must be done on the behavior of different sample and buffer systems in gradients of density, composition, viscosity, conductivity, pH, and field strength.

Before examining some basic equations for migrations we will consider in general terms the implications of a nonuniform flow profile in the horizontal depth direction (z direction) of the apparatus, which has thus far been ignored. The shape of this profile has not been determined experimentally but for a uniform fluid in a thin rectangular slit of width 2c, far from the edge, it would be parabolic,[30] as shown in Fig. 10, with

$$v\left(\frac{cm}{sec}\right) = \left[1 - \left(\frac{z}{c}\right)^2\right] v_{max}, \text{ and } v_{average} = \frac{2}{3} v_{max}. \qquad (33)$$

According to Eq. (33), the fluid in 58% of the cross section would have a linear velocity greater than v_{av} (up to a maximum of 1/2 greater at the center) and in 47% of the cross section, would have a lower velocity (down to zero at the walls).

If this were the case, to the single flow vector v_{av} previously assumed to apply throughout the entire volume, should be added an appropriate variation. The resulting effect on the net migration vectors of Fig. 9 and on the resolution of

---

* Combinations with "chemical forces," e. g., multiphase distribution, making use of the interesting work of Albertsson[45] may prove very fruitful.

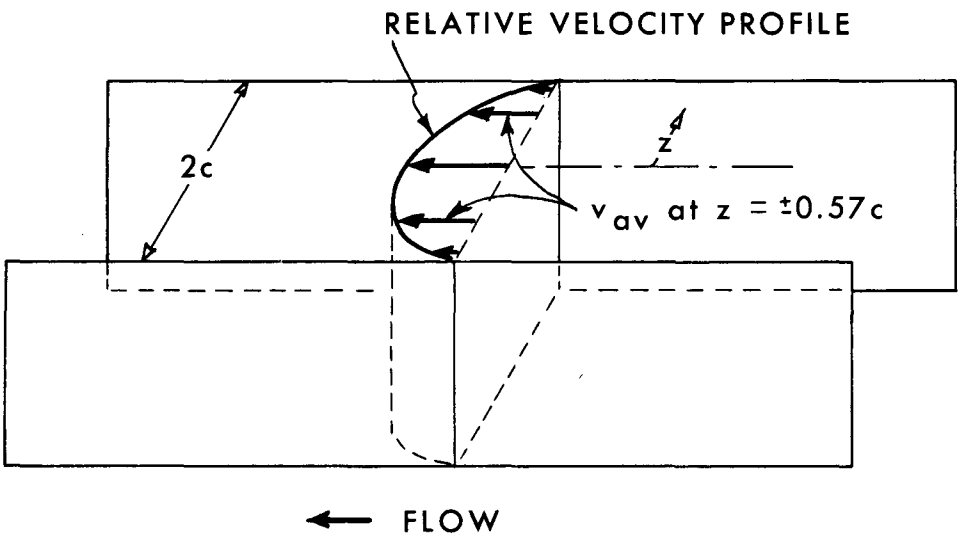

Fig. 10. Ordinary laminar flow through a thin rectangular slit, away from the edges.

components at the outlet would depend on a number of factors. If a similar z-direction variation existed in the vertical migration vectors, some cancellation could occur tending to counteract the change in the resultant migration path. (There would still be a change in length of the resultant vectors but that would not affect the path of a given component through the solution.) Some degree of such cancellation could be expected from vertical parabolic migration profiles in electrophoresis resulting from electroosmotic flow in a closed system,[47,48] but, for general migration cases, this could not be expected.

Under rate-type migration principles (e.g., Fig. 9a) the effect on resolution of this component broadening would be minimized at the outlet if the vertical thickness of the migrating sample band is kept small relative to the outlet spacing, as is usually the case at conductivity barriers. Moreover, for equilibrium migration principles (e.g., Figs. 9c and 9d), the broadening would likely be irrelevant, because the same final position should be reached by a given component regardless of the path of approach.

Whatever the real z dependence of the velocity profile, it has appeared to have relatively little effect on migration paths in STAFLO experiments to date, and a simple two-dimensional vector representation (as in Fig. 9) has appeared satisfactory for expressing the observations both for sedimentation and electrophoresis using molecules and cells, and under both equilibrium and rate migration conditions. Consequently, the uniform-flow assumption will be retained for the remaining discussion in this paper. For highest resolution and greatest flexibility in choice of experimental parameters, however, as well as for the best understanding of the nature of STAFLO flow, more direct knowledge of the z-direction velocity dependence is desirable. (One of the simplest methods of specifying this dependence may be to impose the boundary condition $v(z) \approx$ constant, by use of the two-dimensional outlet pattern referred to above, taking advantage of the same hydrodynamic stability principles used in the vertical direction.)

B. Elementary Transport Relations

1. Cell Sedimentation

An ideal isolated spherical particle with radius r, suspended in a uniform liquid medium and subject to the acceleration of gravity, g, experiences an inertial force in the downward (i.e., x) direction of $4/3\pi r^3 (\rho_p - \rho_m)g$ where ρ_p and ρ_m are densities of the solvated migrating particle and liquid medium respectively. The sedimenting particle encounters a velocity-dependent Stokes frictional force

of $6\pi\eta r\frac{dx}{dt}$ where η is the viscosity of the liquid. For mechanical equilibrium, which is generally quickly established, these two forces are equated yielding the familiar relation for steady sedimentation velocity:

$$\frac{dx}{dt} = \frac{2}{9}\frac{r^2}{\eta}(\rho_p - \rho_m)g. \tag{34}$$

The analytical and preparative interests in this equation, or in similar ones, are closely related. On the one hand, they should determine size or density from measured sedimentation velocities and one additional independent measurement or relation. On the other hand, from the integrated form of the equation, the relation of migration-distance differences Δx_i to STAFLO apparatus outlet spacings defines the sedimentation velocity resolution available after any time t, for collecting separate classes of particles with differing r's and ρ's.

There are a number of difficulties in using equation (34) in a precise quantitative manner for sedimentation of cellular suspensions and even more difficulty in using the integrated forms, arising partly because of our ignorance of the exact values of the parameters and partly from inadequacies in the equation itself. For one thing, corrections should be made for nonspherical shape, both to the $4/3\pi r^3$ volume term and to the frictional term. During sedimentation in various gradients, cell shape or size may change and cell density is not necessarily a well-defined quantity, constant in time. For example, Burns[49] was unable to float yeast cells (Saccharomyces cerevisiae) of presumed density 1.06 or 1.07[50,51] in up to 80% sucrose solutions or in other high density solutions. Of course, cells do not necessarily sediment as individual particles as pointed out previously but may associate or "stick" together for some or all of the time as in the "bombing" previously described or in rouleau formation or other agglomeration phenomena in blood cell sedimentation.[52]

General discussions on differential and integrated forms of the sedimentation equation, especially for higher centrifugal fields, have been given by Svedberg and Pederson,[53] and many others.[2,54,55] Recent reviews especially pertinent to cellular and subcellular particle (gradient) centrifugation are by de Duve, Berthet and Beaufay,[56] and Allfrey.[5] The integration of the sedimentation equation has been discussed by de Duve et al. for a variety of configurations and functional dependences of solution density, composition, and viscosity; particle shape, size, and density; degree of dispersion; and other factors. However, as pointed out by Allfrey,[5] as well as de Duve, the sedimentation properties of heterogeneous cellular mixtures

depend in a complex way on variables not included in the equations (e. g., cell concentrations). For the present purpose, we will neglect the variability of the factors in Eq. (34) and simply use the equation as an approximation for predicting and relating results for STAFLO 1-g sedimentation velocity experiments in small gradients. A future object is to use refined equations based on Eq. (34) to interpret more precisely the measured sedimentation coefficient, which is defined as

$$S = \frac{1}{g}\frac{dx}{dt}, \tag{35}$$

in terms of the more fundamental cellular physical properties (e. g., size, density, shape).

Writing Eq. (34) in the integrated form for two separate components, then subtracting gives

$$(x_2 - x_1) = (x_2 - x_1)_o + \frac{2}{9}\frac{g}{\eta}[r_2^2(\rho_2 - \rho_m) - r_1^2(\rho_1 - \rho_m)]\Delta t, \tag{36}$$

with $(x_2 - x_1)$ the separation of the two components after the sedimentation time Δt and $(x_2 - x_1)_o$ (their initial maximum separation) included to provide for a finite initial sample-band size. Resolution per unit time is favored by a small initial band, capacity by a large one. As an example, let us estimate the time for complete separation in water of two classes of cells of identical density = 1.07 g/cm^3 and radii of 4 and 6 μ respectively, with initial vertical sample band width and outlets spacing of 2.5 mm (apparatus No. 2, Fig. 2). Complete separation distance is taken as 0.25 cm, meaning that this is the smallest vertical migration distance for which non-overlapping fractions can be obtained. This is equivalent to setting $(x_2 - x_1)_o = 0$ and $(x_2 - x_1) = 0.25$, or alternatively $(x_2 - x_1)_o = -0.25$ and $(x_2 - x_1) = 0$. From Eq. (36) we get

$$\Delta t = \frac{(0.25)(9)(0.01)}{(2)(980)(0.07)(36-16)\times 10^{-8}} = 820 \text{ sec} \approx 13.7 \text{ min.}$$

If we wished the stronger condition that all of the larger cells must sediment at least 2.5 mm (1 outlet thickness) farther than any of the smaller cells in this same time, then the time is doubled; i. e., $\Delta t \approx 27$ min. Calculation of the actual distance each will have migrated in 27 minutes shows $x_2 = 9$ mm and $x_1 = 4$ mm (cf. the 30-mm height of the migration chamber in apparatus No. 2). The nominal sedimentation rates of such cells [Eq. (35)] are

$S_1 = 2.5 \times 10^6$, and $S_2 = 5.6 \times 10^6$ Svedberg units (1 Svedberg = 10^{-13} sec).

The parameters for this separation are seen to be comfortably within the capability of the present design of STAFLO apparatus. Of course, physiological cell suspensions are not monodisperse in size as in this example, but polydisperse. However, even where cell-size distributions overlap it has been found possible by use of this sedimentation velocity method to obtain essentually pure fractions from yeast mixtures; good qualitative agreement with the above type calculations is also observed.[39]

Differential migration and separation should also occur, according to Eqs. (34) and (36), for cells of identical size but differing densities. A reasonably good model to test this should be a mixture of nucleated and non-nucleated red cells, and recent experiments in our laboratory with rat bone marrow support this interpretation of their sedimentation.

For equilibrium density sedimentation with strong density (and viscosity) gradients, the time to reach equilibrium as calculated from a corrected and integrated Eq. (34) would generally be much longer, and in fact, such experiments may appear to be precluded. For cells that actually can be brought to density equilibrium, possible experimental ways around this difficulty include:

(a) stopping flow entirely for a time to prolong sedimentation time;

(b) using an appropriately tailored nonlinear density gradient;

(c) using an electric field in the first part of the sedimentation cell to bring the cells rapidly to the vicinity of their density equilibrium positions; and

(d) application of higher acceleration (centrifugal) fields. There appears no a priori reason to exclude this for the STAFLO system although certain engineering problems would have to be worked out. Even a few additional "g" would add greatly to the possibilities for sedimentation experiments with smaller cellular and subcellular particles [cf. Eqs. (34 and (36)].

2. Electrophoresis

If the inertial force used in the derivation of Eq. (34) is replaced by an electrical one, $q\tilde{E}$, where q is the effective particle charge in units of (10^{-7} coulombs) and $\tilde{E}$ is the field strength in volts/cm, we can write corresponding steady-state electrical equations*

$$\frac{dx}{dt}\left(\frac{cm}{sec}\right) = \frac{q\tilde{E}}{6\pi\eta r}, \text{ or } \mu = \frac{1}{\tilde{E}}\frac{dx}{dt} = \frac{q}{6\pi\eta r}, \qquad (37)$$

* The steady state, i.e., "mechanical equilibrium" is established in times of the order of 10^{-14} sec.[57]

where μ is the usual electrophoretic mobility (velocity per unit field strength) in units of cm/sec/volt/cm. Just as the sedimentation constant [Eq. (35)] is primarily related to hydrodynamic, physical parameters of the cell and surroundings, so is μ primarily related to their fundamental electrical parameters, with the relationship, however, somewhat more obscure or at least more controversial.

One can attempt to relate the charge q to the zeta (electric double layer) potential ζ, by the electrostatic expression for a spherical particle; we have

$$\zeta = \frac{q}{\epsilon r} , \tag{38}$$

where ϵ is the dielectric constant of the medium. In the complex ionic environment of ordinary aqueous solutions, both Eqs. (37) and (38) are gross approximations or downright inaccurate representations of the real physical situation. They should be reasonably satisfactory for limiting cases of very low ionic strength where electrostatic shielding becomes unimportant. Substituting Eq. (38) into Eq. (37), taking care to use consistent units,[58] * gives the expression for the mobility:

$$\mu = \frac{\zeta \epsilon}{6\pi\eta} . \tag{39}$$

By some cancellation of errors, Eq. (39) may be approximately valid in more general situations than either Eqs. (37) or (38). However, difficulties remain for using either Eqs. (37) or (39) (or their more sophisticated refinements) to interpret electrophoretic mobility quantitatively in terms of cell charge, zeta potential, surface-charge density, etc. These difficulties are related to such factors as the actual size and shape of the cells, the relation of electrophoretic radius to macroscopic radius, the geometry of the double layer, possible surface conductivity on the cell, the value of the dielectric constant to use in the near vicinity of the cell surface, limitations of the Debye-Hückel theory, etc. A different quantitative analytical property, indirectly based on Eq. (37), that poses no such theoretical difficulty in determination is the isoelectric point. This is simply measured in STAFLO isoelectrically immobilized fractions as the pH of those particular collected fractions for which $\frac{dx}{dt}$ hence q have become equal to zero (e.g., Fig. 9d).

The basic assumptions, limitations, and uncertainties of these electrokinetic derivations have been widely discussed in the literature, as summarized by Bull,[59]

---

* If the dimensionless dielectric constant of cgs units is to be employed, then q must be in esu. If q is in coulombs, the mks dielectric constant must be employed.

McDonald,[60] and by authors in the authoritative book edited by Bier,[61] for example in the article by Overbeek and Lijklema[62] and in the critical review of Brinton and Lauffer.[63] For the present purposes the following dual viewpoint is adopted:

(a) Electrophoretic mobilities and isoelectric points measured under specified conditions are precise physical constants whose atomic and molecular interpretation will become increasingly unambiguous with increased understanding of ionic solution theory, but whose experimental values are of considerable present interest analytically for characterizing state and change of state of cells;

(b) The typical differences in mobilities for different kinds of cells (or cells in different states) are more than adequate to permit large-scale preparative electrophoretic fractionation of cell mixtures (and determination of their mobilities and isoelectric points) by the STAFLO method.

For an analytical (mobility) calculation see Sec. IV. C. We will illustrate the preparative aspect as follows: Writing from Eq. (37)(the definition of μ), we have

$$x - x_o = \int \mu \tilde{E}\, dt,$$

and, for constant μ and $\tilde{E}$ and separate components 1 and 2, we have

$$(x_2 - x_1) = (x_2 - x_1)_o + (\mu_2 - \mu_1)\tilde{E}\, \Delta t, \tag{40}$$

which is an electrophoretic equation analogous to the sedimentation Eq. (36). Considering again 2.5 mm as the "complete separation distance," we find the time for complete separation to be

$$\Delta t\,(\text{sec}) = \frac{0.25}{(\mu_2 - \mu_1)\tilde{E}} \tag{41}$$

In Table III are the times in minutes calculated from Eq. (41) for three experimentally useful field strengths for each of two mobility differences. Except for the combination of lowest $\tilde{E}$ and $\Delta\mu$ the times are all under 45 minutes. Since cellular mobilities and mobility differences are generally of the order of 10^{-4} cm/sec/volt/cm, even low field strengths are sufficient for satisfactorily rapid separations. With proteins, often having mobilities and mobility differences of the order of 10^{-5}, 10 to 50 volts/cm may be desirable. (In STAFLO experiments using such higher field strengths, hemoglobin in the very near vicinity of its isoelectric point has easily been made to migrate 15 mm in 18 minutes.)

Table III. Separation times calculated from Eq. (41).

	$\tilde{E}$ (volts/cm)					
	1		10		50	
	$\mu_2 - \mu_1$		$\mu_2 - \mu_1$		$\mu_2 - \mu_1$	
	10^{-5}	10^{-4}	10^{-5}	10^{-4}	10^{-5}	10^{-4}
t (minutes)	417	41.7	41.7	4.2	8.3	0.83

μ in cm/sec/volt/cm.

The useful increase in mobility with decreasing ionic strength should be pointed out again as it is common to both proteins and cells,[63,64] and it is helpful here in increasing electrophoretic resolution and/or sample capacity. This factor enters into the equations through the Debye-Hückel refinements to Eq. (39).

Since resolution, defined as the $(x_2 - x_1)$ calculated from Eq. (40), increases with decreasing initial sample thickness [e.g., $(x_2 - x_1)_o$], it is sometimes desirable to minimize this initial thickness without changing apparatus. If care is taken to maintain proper density-gradient stability, an initial sample sharpening can easily be brought about by the conductivity barrier migration principle (Sec. IV. A). If the sample-band conductivity is lower than that in the adjacent streams its solutes will become proportionately concentrated into a portion of the initial thickness shortly after the field is applied.*

Throughout such a discussion of variation of electrical parameters we must keep in mind the implications for heat dissipation and make appropriate calculations of the type given in Sec. III. D.3 or of the type made by Bier.[19] Clearly, for use of the highest field strengths with very heat-labile substances, solution conductivities must be kept down or, perhaps, external cooling provided.

3. Combined Electrophoresis and Sedimentation:

With living cells as large as a few microns undergoing electrophoretic migration, unless the solution is specifically chosen to prevent it, sedimentation (or possibly flotation) will generally occur with the electrophoresis, a fact of both preparative and analytical interest. Whatever the relative charge (electrophoretic velocity) of a faster and slower sedimenting cell, the electric-field polarity can always be chosen to increase the separation of the cells in a given time as illustrated in Fig. 11a and 11d. Similarly, we can readily find which of the two is relatively more positively charged by determining whether reversal of electric polarity leads to an increased resultant differential migration (Fig. 11d compared with 11b) or decreased resultant differential migration (Fig. 11c compared with 11a).

---

* Without changing the flow-cell but using a subdivided syringe arrangement, it was also possible to introduce sample into 1/2 or 1/3 of the usual 2.5-mm layer.

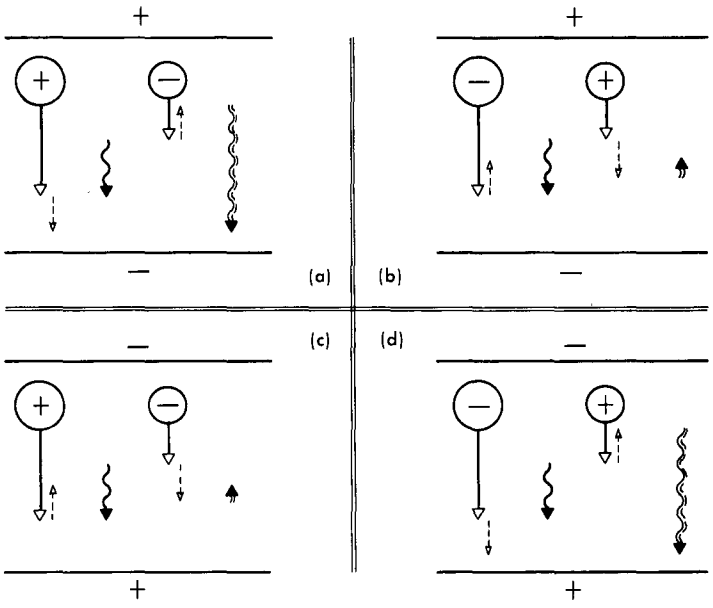

SOLID ARROWS : SEDIMENTATION VELOCITY VECTORS
DOTTED ARROWS : ELECTROPHORETIC VELOCITY VECTORS
SINGLE WAVY ARROWS : SEDIMENTATION DIFFERENCE VECTORS
DOUBLE WAVY ARROWS : RESULTANT DIFFERENCE VECTORS

MU-29024

Fig. 11. Combined sedimentation and electrophoresis of cells.

C. Experimental Systems and Parameters for STAFLO Method: Summary

Electrophoresis in the opposing direction to gravity was reported in experiments with yeast and dye, and yeast and bacteria.[1] A detailed fractionation and pure sedimentation study of a heterogeneous mixed ploidy yeast suspension is being reported.[39] Sedimentation experiments have now been completed on rat bone marrow with fractionation achieved for several nucleated and nonnucleated components; the details will be reported in the near future. Cell migrations have generally been performed with small density gradients (e. g., 0 to 2 to 4% of sucrose or other solute) with cell concentrations of 2 to 5×10^7 cells/cc. Where isotonicity was necessary or desirable, the background solutions were isotonic, with dextran added for density increments. Migration chamber flow rates have been of the order of cc/min/inlet.*

Most of the purely electrophoretic separation and interaction studies to date have been on mixtures of dyes or proteins[1, 7] and have employed these same small density gradients. Even in a smaller 5-in.-long apparatus, initial protein migrations and separations were easily effected.[1] Sample concentrations up to $\approx 0.2\%$ have been used. For scale-up to higher cell concentrations or higher protein concentrations, stronger density gradients will be necessary. Electric-field strengths up to about 100 volts/cm have been employed, though relatively little work has been done above 50 volts/cm. Currents have generally been below 20 mA or 1 mA/cm^2. Steady-state times in the force field have ranged from 2 to 60 minutes with intermediate values generally adopted. One of the problem areas under current investigation is operation at the higher power levels necessary for cell electrophoresis in high conductivity solutions and for larger scale preparative work with natural protein mixtures.

Several types of analytical studies have been shown possible, or indicated, including protein-protein interactions, protein-small-ion interactions, "crossover" reaction experiments, instantaneous determination of time-dependent transport properties (e. g., electrophoretic mobility, diffusion constant).[1, 7]

A photograph illustrating experimentally with dyes several of the points discussed in this paper is given in Fig. 12. A mixed aqueous solution of 0.001% cresyl violet and 0.001% bromphenol blue is entering via inlet No. 7. The two components, which have opposite charge, separate by migrating to the lower and upper positions respectively.

---

* For electrophoresis, sufficiently fast buffer flow through the electrode compartment is chosen to prevent migration of electrode reaction products into the main migration chamber unless this migration is specifically desired (e. g., to help set up a pH gradient).

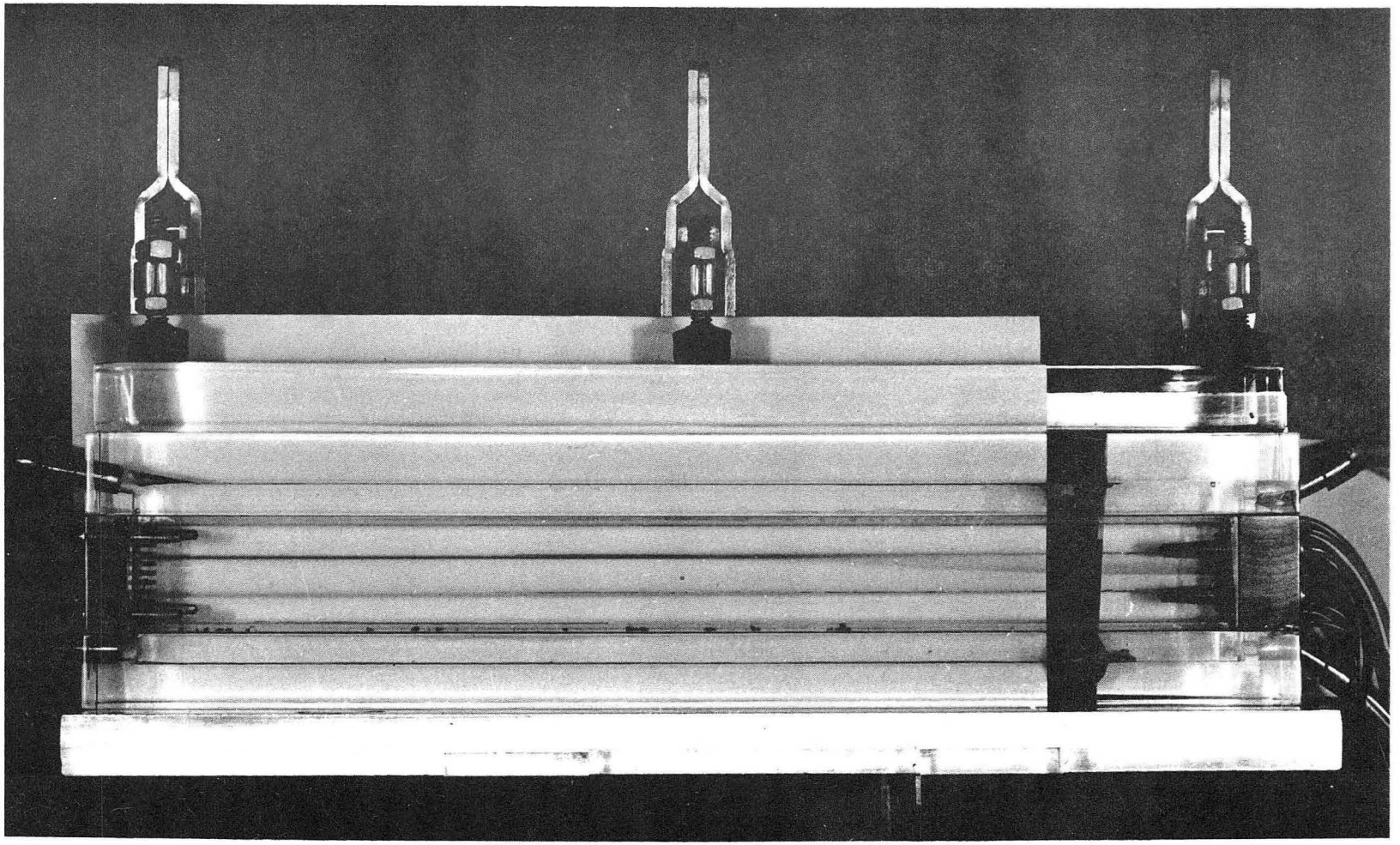

ZN-2339

Fig. 12. Electrophoretic migration and separation of bromphenol blue and cresyl violet.

With a total of 10 volts and a flow rate of 0.45 cc/minute/inlet (11.5 minutes in the apparatus) separation is already complete in about two minutes. The migration illustrated is that of a double-migration barrier through use of conductivity discontinuities (Fig. 9c), the two components having reached their respective barriers in less than five minutes. Inlet solutions 1 to 4 and the top electrode solution are pH4 phthalate buffer, ionic strength 0.001; solutions 9 to 12 and the bottom electrode solution are pH7 phosphate buffer, ionic strength 0.002 with 2% added sucrose. Solutions 5, 6, 7, and 8 contain 0.4%, 0.6%, 0.8%, and 1.0% sucrose, respectively. The lower border of the upward migrating bromphenol blue component is seen darker than the solution directly below, with the slope of this migration border being a measure of the electrophoretic velocity of the component, which (at constant field strength) is proportional to its mobility. In this earlier form of the apparatus the electrode did not extend all the way to the inlet (right)* so field strength just beyond the inlet is very low. The above mentioned slope is thus approximately zero in this region, increasing to a value ≈ 0.07 during the uniform upward migration phase, then dropping abruptly to zero at the "migration barrier." For a rough estimate of the mobility, we can write the slope as $0.07 \times \frac{\text{vertical cm}}{\text{horizontal cm}}$; at this flow rate, 30 horizontal cm = 11.5 minutes or 690 sec. With most of the 10-volt drop appearing across the low-conductivity middle centimeter of the apparatus we can write, for the field strength in this region, $\tilde{E} \approx 8$ volts/vertical cm. We, therefore, estimate $\mu \approx \frac{(0.07)(30)}{(8)(690)} = 4 \times 10^{-4}$ cm/sec/volt/cm, a reasonable value. If care is taken to adjust the electrical conductivities of solutions properly before introducing them, then these components, and others in multicomponent mixtures, can be made to migrate essentially as individual bands having vertical thickness approx. equal to the inlet band height (here 2.5 mm), according to the mobility-difference migration principle (Fig. 9b).

---

*Although it has not yet been noted in STAFLO experiments, there may be stability advantage in this geometry, which allows some gradient smoothing diffusion for entering streams before they reach the region of high electric field; this is analogous to Svensson's suggestions for nonflow density-gradient columns.[15]

APPENDIX

A. Definitions and Basic Concepts

Flow pattern. The instantaneous "picture" of the flowing streams inside the main migration chamber (e. g., Figs. 3 and 7, plate I).

Steady state (especially referring to the flow pattern). The time-independent condition of flow pattern. A steady-state pattern may be in a "normal" geometrical position as in Fig. 3, or it may be displaced.

Drift (of flow pattern). The change of flow pattern when it is not in a steady state.

Hydrostatic balance or equilibrium (sometimes, just equilibrium). The instaneous condition with the individual liquid heights in the collection bottles (i. e., the ℓ's) satisfying the basic hydrostatic Eqs. (6) and (14) (as given in Table I, Fig. 5, etc.)

Crossover point. A point of intersection of any 2 lines plotted as in Fig. 5, especially those for the 12 collection-fraction case. In Fig. 5 itself, the single such point occurs at the 100% coordinates.

Feedback. Used primarily in the "negative" or self-balancing sense, referring solution outflows or collection-bottle liquid levels.

Stable. Applying to level configuration or steady-state condition; implies that perturbations to the instantaneous level configuration or flow pattern are damped out (by the feedback).

Solution No. i. The particular solution entering via inlet No. i.

Inflow rate No. i. The flow rate of liquid entering via inlet No. i, i. e., Q_i^{in}. This is the same as inflow or input rate of solution No. i, i. e., $Q_{soln\ i}^{in}$ from the physical relationship of the pumps to the flow-cell.

Outflow rate No. i. The flow rate of liquid exiting via outlet No. i, i.e., $Q_i^{out} = \sum_{all\ soln\ j} (Q_i^{out})_j$. This is not necessarily the same as outflow or output rate of solution No. i, $Q_{soln\ i}^{out}$, which represents the total outflow of solution i by whatever outlet, i. e., equal to $\sum_{all\ outlets\ j} (Q_{soln\ i}^{out})_j$.

B. Glossary

Symbol	Units	Definition; where first found
a	(cm)	half height of rectangular conduit; Eq. (25)
A, A_1, A_6	(cm^2)	areas; Eq. (29), Sec. III. C.2, Fig. 6
c	(cm)	half horizontal depth of rectangular conduit Eq. (25); Fig. 6; Eq. (33); Fig. 10
c_i, Δc_i		concentration and concentration increment of ith component; Eq. (28)
c(x)	(g/cm)	concentration distribution in a gradient column; see the Eq. preceding Eq. (32)
$\tilde{c}_p$	(cal/g·°C)	specific heat capacity; Eq. (31)
C		constant; Eq. (23)
d	(cm)	vertical height of main migration chamber; Eq. (3); Fig. 4
D_1, D_i		diffusion coefficient for principle solute, for ith component; Eq. (28)
$\tilde{E}$	(volts/cm)	electrical field strength; Eq. (30); Eq. (37)
g		acceleration of gravity; Sec. I; Eq. (2)
h	(cm)	apparatus parameter; Eq. (1); Fig. 4.
		height of specified volume of solution; see the equation preceding Eq. (32)
i		running index
i	(amps)	electrical current; Eq. (29)
$\tilde{i}$	($amps/cm^2$)	current density; Eq. (30)
i. d.		"inside diameter"
j		running index
k	($ohm^{-1}cm^{-1}$)	specific conductivity; Eq. (29)
ℓ, ℓ_1, ℓ_2, $\cdots \ell_i$	(cm)	collection-bottle liquid heights; Eq. (1); Fig. 4
ℓ_1^*, ℓ_2^*, $\cdots$	dimensionless	relative values of ℓ's, $= \frac{\ell_1}{M} \times 100$, $\frac{\ell_2}{M} \times 100 \cdots$; Table I; Fig. 5

$m_1, m_2, \cdots m_i$	dimensionless	positions of outlets Nos. 1, 2, $\cdots$ i $\cdots$ measured as a fraction of d; Eq. (13), Fig. 4
M	(cm)	apparatus parameter, $= (h - \frac{d}{2})$; Eq. (6), Fig. 4
$M_1, M_2 \cdots M_i$	(cm)	apparatus parameter applicable for general linear density functions $\rho(x)$; $M_i = (h - \frac{m_i d}{2})$; Eq. (14), (15); for 12 fractions, $M_{12} = M$, Eq. (15) and following
$\underline{m}$, $\underline{m}_2$	(g)	stable mass in specified portion of gradient column; Eq. (32) and preceding equation
n		running index; Eq. (25)
0		outlet position; Fig. 9 and Sec. IV. A
p, p'		positions of migration barriers; Fig. 9 and Sec. IV. A
P		pressure; Eq. (25)
q	(10^{-7}coulombs)	effective particle charge; Eq. (37)
Q, Q_1, Q_6	(cm^3/sec)	volume flow velocities; Eq. (22); following Eq. (24)
Q_i^{in}, Q_i^{out}	volume/time	liquid flow rate moving through inlet i or outlet i; $Q_i^{out} = \sum_{\text{all solution } j} (Q_i^{out})_j$; Sec. III. B. 1, Eq. (8)
$Q_{\text{soln i}}^{in}$	volume/time	flow rate of solution i entering the flow-cell (necessarily via inlet i) Secs. III. B. 1 and 2; Eq. (18)
$Q_{\text{soln i}}^{out}$	volume/time	flow rate of solution i exiting from the flow-cell, not necessarily via any one or more outlets; $Q_{\text{soln i}}^{out} = \sum_{\text{all outlets } j} (Q_{\text{soln i}}^{out})_j$ Secs. III. B. 1 and 2; Eq. (18)
r	(cm)	radial distance from center of pipe; Eq. (21)
	(cm)	radius of spherical particle; Eq. (34)
	(ohm-cm)	specific resistivity; Eq. (29) and footnote following
R	(cm)	mean hydraulic radius; Eq. (20)
	(cm)	radius of circular pipe; Eq. (21); Fig. 6
	(ohms)	electrical resistance; footnote following Eq. (29)

Re	dimensionless	Reynolds number; Eq. (20)
S, S_1, S_2	(Svedbergs $= 10^{-13}$ secs)	sedimentation coefficients; Eq. (35); Sec. IV. B. 1
STAFLO		short for "stable-flow free boundary"
t	(sec)	time; Eq. (28); Eq. (34); Eq. (37)
Δt	(sec)	duration of complete separation; Eq. (36); Eq. (40)
T, Δ T	(°C)	temperature, temperature rise; Eq. (31); Table II
v; v_r	(cm/sec)	linear flow velocity; as a function of radial distance r; Eq. (20); Eq. (21)
V	(cm^3)	main migration chamber volume; Eq. (31)
	(cm^3)	a solution volume; Eq. (32)
$V_1, V_2, \cdots V_i \cdots$	(cm^3)	volume of liquid in collection bottles; Sec. III. B. 1, Fig. 5
$\bar{v}_2$, $\bar{v}_i$		partial specific volume of solute, ith component; Eq. (32); Eq. (28)
w	(watts)	power dissipated; Eq. (29)
$\tilde{w}$	(calories/cm^3)	intensive unit of power dissipation; Eq. (30)
x	(cm)	vertical distance coordinate; Eq. (2), Fig. 4; Eq. (22), Fig. 6; Eq. (26), Fig. 8; footnote following Eq. (29); Eq. (34)
x_1, x_2	(cm)	specific values of x; Eq. (22)
	(cm)	migration distances for components 1 and 2; Eq. (36); Eq. (40)
$(x_2 - x_1)_o$	(cm)	initial separation of components 1 and 2 (band size); Eq. (36); Eq. (40)
Δx_i	(cm)	the ith migration distance difference; following Eq. (34)
y	(cm)	horizontal coordinate; Eq. (25)
z	(cm)	horizontal depth coordinate; Eq. (22), Fig. 6; Eq. (33), Fig. 10
ϵ	(ϵ)	dielectric constant; Eq. (38); footnote following Eq. (38)

ζ		zeta potential; see Eq. (38)
η	(poise = $\frac{g}{cm\text{-}sec}$)	absolute viscosity; Eq. (20)
μ, μ_1, μ_2	($\frac{cm^2}{sec\text{-}volts}$)	electrophoretic mobility; Eq. (37); Eq. (40); Table III
ρ_1 $\rho(x)$	(g/cm^3)	density function in flow-cell just before outlet; Eq. (2), Fig. 4
	(g/cm^3)	solution density in a gradient column; Eq. (28), Fig. 8
ρ_o	(g/cm^3)	solvent density in a gradient column; Eq. (28), Fig. 8
$\rho_1, \rho_2, \cdots \rho_i \cdots$	(g/cm^3)	densities of entering streams; Eq. (2), Fig. 4 Sec. III. D. 2, Fig 8
ρ_p	(g/cm^3)	density of solvated particle; Eq. (34)
ρ_m	(g/cm^3)	density of liquid medium; Eq. (34)
$\Delta\rho_o$	(g/cm^3)	density difference across specified solution height h; Eq. (32)
$\Delta_w\rho$	(g/cm^3)	smallest density difference stably compatible with $\tilde{w}$; Eq. (32)

ACKNOWLEDGMENTS

This work was partially performed under U. S. Public Health Service Grant HF 4941. The support of the U. S. Atomic Energy Commission, Lawrence Radiation Laboratory, is also gratefully acknowledged. I am indebted to several associates, particularly C. A. Tobias, M. J. Polissar, and R. M. Glaeser for careful reading of the manuscript and numerous helpful criticisms.

REFERENCES

1. Howard C. Mel, University of California Lawrence Radiation Laboratory Report UCRL-9108, 1960.
2. N. G. Anderson, in G. Oster and A. W. Pollister, Eds. Physical Techniques in Biological Research, Cells and Tissues (Academic Press, New York, 1956), Vol. III, pp. 299-352.
3. M. Behrens, "Zell und Gewebtrennung," in E. Abderhalden, Ed., Handbuch der biologischen Arbeitsmethoden, Abt. 5, Teil 10:2, (Urban and Schwarzenberg, Berlin, 1938), 1363-1392.
4. P. E. Lindahl, Biochim. et Biophys. Acta 21, 411-15 (1956).
5. V. Allfrey, in J. Brachet and A. Mirsky, Eds., The Cell (Academic Press, New York, 1959), Vol. I, pp. 193-290.
6. Howard C. Mel, J. Chem. Phys. 31, 559 (1959).
7. Howard C. Mel, Science 132, 1255-6 (1960).
8. Revco, Inc., 1900 Lyndale Ave. So., Minneapolis 5, Minn.
9. W. G. Cutler, Am. J. Phys. 27, 185 (1959).
10. Roger Gilmont Instruments, Inc., Great Neck, N. Y.
11. Daystrom, Inc., Benton Harbor, Michigan.
12. A. Tiselius, Trans. Faraday Soc. 33, 524-31 (1937).
13. S. Raymond, Science 128, 1462 (1958).
14. R. Dobry and R, K. Finn, Chem. Eng. Progr. 54, 59 (1958).
15. H. Svensson, "Zonal Density Gradient Electrophoresis," in P. Alexander and R. J. Block, Eds., Analytical Methods of Protein Chemistry (Pergamon Press, New York, 1960), Vol. I, pp. 193-244.
16. J. St. L. Philpot, Trans. Faraday Soc. 36, 38-46 (1940).
17. M. Bier, in M. Bier, Ed., Electrophoresis (Academic Press Inc., New York, 1959), pp. 263-315.
18. R. K. Finn, in H. M. Schoen, Ed., New Chemical Engineering Separation Techniques (Interscience Publishers, Inc., New York, 1963).
19. M. Bier, in S. P. Colowick and N. O. Kaplin, Eds. Methods in Enzymology (Academic Press, Inc., New York, 1962), Vol. 5, pp. 33-50.
20. E. Schumacher and R. Flühler, Helv. Chim. Acta 41, 1572-81 (1958).
21. M. Bier, Science 125, 1084 (1957).
22. J. Barrollier, E. Watzke, and H. Gibian, Z. Naturforsch. 13B, 754-55(1958).
23. K. Hannig, Z. Anal. Chem. 181, 244-54 (1961).

24. H. Wolffgang, Institut fur Phytopathologie Aschersleben der Biologischen Zentralanstalt der Deutschen Academie der Landwirtschaftwissenschaften zu Berlin, Tagungsberichte 33, 93-100 (1961).
25. A. Kolin, Proc. Natl. Acad. Sci. U.S. 46, 509-523 (1960).
26. The Physical Treatises of Pascal, translated by I. H. B. and A. G. H. Spiers (Columbia University Press, New York, 1937).
27. Becton, Dickinson, & Co., Rutherford, New Jersey.
28. R. B. Bird, W. E. Stewart, and E. N. Lightfoot, Transport Phenomena (John Wiley & Sons, Inc., New York, 1960).
29. T. B. Drew, H. H. Dunkle, and R. P. Genereaux, "Flow of Fluids," in J. H. Perry, Ed. Chemical Engineers Handbook 3rd edition (McGraw-Hill Book Co., Inc., New York, 1950), pp. 369-396.
30. Reference 28, chapter 2.
31. R.J. Cornish, Proc. Roy. Soc. (London) A120, 691-700 (1928).
32. J. Nikuradse, Ingr. Arch. 1, 306-332 (1930).
33. G. Murphy, Mechanics of Fluids, 2nd edition (International Textbook Co., Scranton, Pennsylvania, 1952), pp. 146-49.
34. H. Rouse, Fluid Mechanics for Hydraulic Engineers (McGraw Hill Book Co., Inc., New York, 1938), p. 267.
35. A. Kolin, Biochim. et Biophys. Acta 32, 538-43 (1959).
36. H. Svensson, L. Hagdahl, and K. D. Lerner, Sci. Tools, 4, 1-10 (1957).
37. M. K. Brakke, Arch. Biochem. Biophys. 55, 175-190 (1955).
38. A. Kolin, J. Chem. Phys. 23, 407(L) (1955).
39. Howard C. Mel, Stable-Flow Free Boundary (STAFLO) Migration and Fractionation of Cell Mixtures, IV: Sedimentation Separation of a Mixed Ploidy Yeast Population (in preparation).
40. R. R. Williams and R. E. Waterman, Proc. Soc. Exp. Biol. Med. 27, 56 (1929).
41. A. Kolin, in D. Glick, Ed., Methods of Biochemical Analysis (Interscience Publishers, Inc., New York, 1958), Vol. VI, pp. 259-88.
42. W. G. Kauman, Acad. Roy. Belg. Bull. Classe. Sci. 43, 854-68 (1957).
43. H. Svensson, Acta. Chem. Scand. 15, 325-41 (1961); 16, 456-66 (1962); Arch. Biochem. and Biophys., Supp. 1, 132-38 (1962).
44. E. Schumacher, Helv. Chim. Acta 40, 2322-40 (1957).
45. P. Albertsson, Partition of Cells and Macromolecules (John Wiley & Sons, Inc.), New York, 1960).
46. A. Kolin and R. T. Kado, Nature 182, 510-12 (1958).

47. R. Ellis, Z. physik. Chem. 78, 321-52 (1912).
48. H. A. Abramson, Electrokinetic Phenomena and Their Application to Biology and Medicine, Amer. Chem. Soc. Monograph series (The Chemical Catalog Co., Inc., New York, 1934).
49. V. Burns, University of California Radiation Laboratory Report UCRL-2812 (Thesis), 1954.
50. K. C. Brace, Proc. Soc. Exp. Biol. Med. 74, 751-5 (1950).
51. S. Aiba, S. Kitai, and N. Ishida, Hakko Kogaku Zasshi (J. Ferm. Technol.) 40, 70-7 (1962).
52. M. M. Wintrobe, Clinical Hematology, 5th edition (Lea & Febiger, Philadelphia, 1961).
53. T. Svedberg and K. O. Pederson, The Ultracentrifuge, (Oxford University Press, London, 1940).
54. H. K. Schachman, Ultracentrifugation in Biochemistry (Academic Press, New York, 1959).
55. H. Fujita, Mathematical Theory of Sedimentation Analysis (Academic Press, New York, 1962).
56. C. de Duve, J. Berthet, and H. Beaufay, Progr. Biophys. Biophys. Chem. 9, 326-69 (1959).
57. R. Audubert and S. de Mende, The Principles of Electrophoresis (The Macmillan Company, New York, 1960).
58. R. J. Hunter, J. Colloid Sci. 16, 190-2 (1961).
59. H. B. Bull, Physical Biochemistry 2nd edition (John Wiley & Sons, Inc., New York, 1951), Chap. 9.
60. H. J. McDonald, in E. Heftmann, Ed., Chromatography (Reinhold Publishing Corporation, New York, 1961), pp. 207-41.
61. M. Bier, Ed., Electrophoresis (Academic Press, New York, 1959).
62. J. Th. G. Overbeek and J. Lijklema, "Electric Potentials in Colloidal Systems," in reference 61, pp. 1-33.
63. C. C. Brinton, Jr. and M. A. Lauffer, "The Electrophoresis of Viruses, Bacteria, and Cells, and the Microscope Method of Electrophoresis," in reference 61, pp. 427-92.
64. A. Tiselius and H. Svensson, Trans. Faraday Soc. 36, 16-22 (1940).